

1 **Atmospheric processes of organic pollutants over a remote lake**
2 **of the central Tibetan Plateau: Implications for regional cycling**

3

4 Jiao Ren^{1,3}, Xiaoping Wang^{1,2,*}, Chuanfei Wang^{1,2}, Ping Gong^{1,2}, and Tandong Yao^{1,2}

5

6 ¹Key Laboratory of Tibetan Environment Changes and Land Surface Processes,
7 Institute of Tibetan Plateau Research, Chinese Academy of Sciences, Beijing, 100101,
8 China

9 ²CAS Center for Excellence in Tibetan Plateau Earth Sciences, Beijing, 100101,
10 China

11 ³University of Chinese Academy of Sciences, Beijing 100049, China

12

13

14

15

16 * **Corresponding author.**

17 (X. Wang)

18 E-mail: wangxp@itpcas.ac.cn

19 Tel: +86-10-84097120

20 Fax: +86-10-84097079

21 **Abstract**

22 Atmospheric processes (air-surface exchange, and atmospheric deposition and
23 degradation) are crucial for understanding the global cycling and fate of organic
24 pollutants (OPs). However, such assessment over the Tibetan Plateau (TP) remains
25 uncertain. More than 50% of the Chinese lakes is located on the TP, which exerts a
26 remarkable influence on the regional water, energy, and chemical cycling. In this
27 study, air and water samples were simultaneously collected in Nam Co, a large lake
28 on the TP, to test whether the lake is a “secondary source” or “sink” of OPs. Lower
29 concentrations of organochlorine pesticides (OCPs) and polychlorinated biphenyls
30 (PCBs) were observed in the atmosphere and lake water of Nam Co, while the levels
31 of polycyclic aromatic hydrocarbons (PAHs) were relatively higher. Results of
32 fugacity ratios and chiral signatures both suggest that the lake acted as the net sink of
33 atmospheric hexachlorocyclohexanes (HCHs), following their long-range transport
34 driven by the Indian Monsoon. Different behaviors were observed in the PAHs, which
35 primarily originated from local biomass burning. Acenaphthylene, acenaphthene, and
36 fluorene showed volatilization from the lake to the atmosphere; while other PAHs
37 were deposited into the lake due to the integrated deposition process (wet/dry and
38 air-water gas deposition) and limited atmospheric degradation. As the dominant PAH
39 compound, phenanthrene exhibited a seasonal reversal of air-water gas exchange,
40 which was likely related to the melting of the lake ice in May. The annual input of
41 HCHs from air to the entire lake area (2015 km²) was estimated as 1.9 kg year⁻¹, while
42 those estimated for \sum_{15} PAHs can potentially reach up to 550 kg year⁻¹. This study
43 highlights the significance of PAH deposition on the regional carbon cycling in the
44 oligotrophic lakes of the TP.

45 **1. Introduction**

46 Since the past century, large quantities of organic pollutants (OPs), such as
47 organochlorine pesticides (OCPs), polychlorinated biphenyls (PCBs), and polycyclic
48 aromatic hydrocarbons (PAHs), have been discharged into the global environment.
49 Soils, water bodies, and snow/ice are generally considered as reservoirs or sinks of
50 these pollutants (Dalla Valle et al., 2005; Froescheis et al., 2000; Guglielmo et al.,
51 2012). However, due to the influence of global warming (Komprda et al., 2013;
52 Noyes et al., 2009), growing evidence indicates that OPs previously stored in
53 reservoirs can be re-released back to the environment (Ma et al., 2011). For example,
54 air-soil exchange of OCPs has showed the re-emission of OCPs from past
55 contaminated soils in Europe (Ruzickova et al., 2008), North America (Kurt-Karakus
56 et al., 2006), and India (Chakraborty et al., 2015). Modeling results have suggested
57 that large parts of the global ocean have been losing dichlorodiphenyltrichloroethane
58 (DDT) via volatilization (Stemmler and Lammel, 2009). In addition, air-sea exchange
59 of PAHs has revealed that the seawater in the Mediterranean has turned into a
60 temporary secondary source of PAHs, which is related to biomass burning in that
61 region (Mulder et al., 2014). Moreover, melting ice and glaciers also have released
62 OPs back into the atmosphere, which buffers the decline of OP levels in the polar
63 regions (Ma et al., 2011; Geisz et al., 2008).

64 Similar to the polar regions, the Tibetan Plateau (TP) has been regarded as a
65 “convergence” of OPs (Wang et al., 2016). Due to the continuous use of OPs in the
66 surrounding countries and the “cold trapping” by the TP, the enrichment of OPs in the
67 TP environment has been reported (Sheng et al., 2013; Wang et al., 2015). However,
68 the TP has experienced great warming (Liu and Chen, 2000), and results of the air-soil
69 exchange of OPs have indicated that the Tibetan soils are acting as a sink of DDT and
70 higher molecular weight PAHs, but are a potential secondary source for
71 hexachlorobenzene (HCB) and hexachlorocyclohexanes (HCHs) (Wang et al., 2014;
72 Wang et al., 2012). This shows that the cold temperature over the TP might not be
73 sufficient to trap volatile OPs. More studies on the air-surface exchange of OPs over

74 the TP are therefore needed to test the role of the terrestrial and aquatic ecosystems of
75 the TP in the regional cycling of OPs.

76 Known as “Asia’s water power”, the TP contains the headwaters of many major rivers
77 in Asia, which provide water sources for about one-sixth of the world’s population
78 (Yao et al., 2012). The TP also has large numbers of remote lakes that are important
79 components of water bodies. Low temperature, oligotrophic conditions, and the long
80 duration of ice-cover are distinct features of these lakes. Based on the higher
81 atmospheric concentrations of α -HCH in summer, Xiao et al. (2010) deduced that
82 these enhanced concentrations may be caused by the thawing of lake ice, which
83 promotes the re-evaporation of α -HCH. However, the study did not include
84 measurements of HCH levels in lake water or the corresponding air-water exchange
85 analysis (Xiao et al., 2010). Therefore, it is still unclear whether the lake water of the
86 TP is the secondary source of a large number of OPs. Furthermore, biomass burning is
87 a widespread activity over the TP (Hu et al., 2015). A recent study demonstrated that
88 the locally sourced biomass combustion particles contributed substantially to the
89 black carbon (BC) loading of the TP glacier (Li et al., 2016). Given that PAHs and BC
90 both mainly originate from incomplete combustion of biomass, regional air-water
91 exchange of PAHs would also contribute to the overall air-surface exchange of
92 carbon.

93 We therefore conducted air and water sampling in a remote lake on the TP, and
94 assessed the air-water gas exchange, and the dry and wet deposition processes of
95 OCPs, PCBs, and PAHs. The aims of this study were to ascertain whether the Tibetan
96 lake represents a secondary source of OPs, to investigate the influence of seasonal
97 lake ice melting on the gas exchange of different OPs, and to estimate the contribution
98 of PAH exchange to the lake carbon budget.

99 **2. Materials and methods**

100 **2.1 Site description**

101 Nam Co Lake (30°30′–30°56′N, 90°16′–91°01′E, 4718 m) is located in the north of

102 the Nyainqentanglha Mountains, on the central TP (Figure 1). It is the second largest
103 lake in Tibet with an area of 2015 km² and a maximum depth exceeding 90 m (Wang
104 et al., 2009). The lake is mainly supplied by precipitation and glacier meltwater.
105 Annual riverine delivery of water to the lake is approximately 1.3×10⁹ m³ year⁻¹,
106 while there is no outflow (Wu et al., 2014). The lake water is alkaline (pH=9.21) and
107 slightly saline (Wang et al., 2009). The climate of Nam Co is relatively cold and
108 windy with an annual average temperature of ~0 °C and an annual wind speed of ~4
109 m/s. The regional climate also has large seasonal variation: the Indian Monsoon
110 dominates summer (May to September) and the westerlies control winter climate
111 (October to April) [see the Supplement (S), Figure S1]. High temperatures and
112 precipitation are usually observed in summer (Figure S2), and the lake begins to thaw
113 from the beginning of May and melts completely by the end of May, which coincides
114 with the onset of the Indian Monsoon. During the winter, the lake is covered by ice
115 due to the subzero temperatures (Figure S2) and maximum instantaneous wind speeds
116 reaching up to 9.9 m/s.

117 The dominant land cover in Nam Co is alpine steppe and meadow, and the local
118 residents herd yak and sheep that graze around the lake. Biomass burning occurs for
119 heating, cooking, transport, and religious reasons. Near the southeastern shore, the
120 Nam Co Monitoring and Research Station for Multisphere Interactions (NCMORS) is
121 operated by the Chinese Academy of Sciences (Figure 1b). This station not only
122 facilitates the consecutive collection of field samples used in the current study, but
123 also provides local meteorological parameters for flux calculations.

124 **2.2 Air and water sampling**

125 An active air sampler (AAS) was deployed on the roof of NCMORS (Figure 1b) and
126 the air monitoring was conducted for two consecutive years from September 2012 to
127 September 2014. The flow rate of AAS was 60 L min⁻¹ and the air samples were
128 collected every 2 weeks with a volume of approximately 600 m³ for each sample. The
129 air stream passes first through glass fiber filters (GFFs 0.45 μm, Whatman) to collect
130 the total suspended particles (TSP) and then through polyurethane foam (PUF, 7.5×6

131 cm diameter) to retain the OPs in gas phase. In total, 47 air samples were collected.
132 Details regarding the sampling period, average air temperature, and wind speed are
133 given in Table S1. All harvested PUF and GFFs were stored at -20 °C until extraction.

134 To determine the OP levels in water, two sampling programs were conducted. First,
135 15 sites around the Nam Co Lake (surface lake water, 0–1 m depth) were selected to
136 obtain the spatial distribution of OPs in lake water (Figure 1b), which provides a
137 direct over-view of OP contamination over the lake. Second, monthly water samples
138 were collected at a site close to NCMORS (Figure 1b) from May to September, 2014
139 (water samples were not obtained during winter due to the ice cover). This provided
140 information regarding temporal variations in OP levels, isomer ratios, and the
141 enantiomeric fraction in lake water. Furthermore, coupled with the monthly average
142 air concentrations of individual OPs obtained, this allowed us to investigate the
143 air-water gas exchange of OPs (direction, flux, and monthly variations).

144 Water samples (200 L) were filtered with GFFs (0.7 µm, Whatman) to obtain the total
145 suspended particulate matter (SPM), and then pumped through an XAD-2 resin
146 column to collect the dissolved phase compounds. For each sampling month, triplicate
147 samples were collected. In total, 15 samples for the spatial study and 15 samples for
148 the temporal study were collected. XAD columns were kept at 4 °C until extraction.
149 The lake water properties (temperature, pH and salinity) are provided in Table S2.

150 **2.3 Sample extraction and analysis**

151 The chemical extraction and cleanup methods are detailed in Text S1 for each sample
152 type [air (PUF plug), TSP, water (XAD column), and SPM]. OPs were analyzed on a
153 gas chromatograph with an ion-trap mass spectrometer (GC-MS, Finnigan Trace
154 GC/PolarisQ) operating under MS–MS mode. More information on the
155 chromatographic conditions is given in Text S2. The target compounds are as follows:
156 HCHs (including α -HCH, β -HCH, and γ -HCH), HCB, DDTs (*o,p'*-DDE, *p,p'*-DDE,
157 *o,p'*-DDT, and *p,p'*-DDT), PCBs (PCB 28, PCB 52, PCB 101, PCB 138, PCB 153,
158 and PCB 180), and 15 priority PAHs listed by the United States Environment

159 Protection Agency (USEPA, without naphthalene), including acenaphthylene (Acel),
160 acenaphthene (Ace), fluorene (Flu), phenanthrene (Phe), anthracene (Ant),
161 fluoranthene (Fla), pyrene (Pyr), benz[a]anthracene (BaA), chrysene (Chr),
162 benzo[b]fluoranthene (Bbf), benzo[k]fluoranthene (Bkf), benzo[a]pyrene (BaP),
163 dibenz[a, h]anthracene (DahA), benzo[g, h, i]perylene (BghiP), and
164 indeno[1,2,3-cd]pyrene (IcdP). Enantiomers of α -HCH were determined with a
165 BGB-172 chiral column (see Text S2 for details). The chiral signature of α -HCH is
166 expressed using the enantiomeric fraction (EF), which is equal to the ratio of peak
167 areas of the (+)/[(+) + (-)] (Harner et al., 2000).

168 **2.4 Quality assurance/quality control (QA/QC)**

169 All analytical procedures were monitored using strict QA/QC measures. Prior to
170 sampling, PUF and XAD resin were pre-cleaned using dichloromethane (DCM) for
171 16 h and GFFs were baked at 450 °C for 4 h. Six PUF field blanks, three XAD field
172 blanks, and six procedural blanks were prepared; HCB, Phe, Ant, Fla, and Pyr were
173 detected in the field blanks (Table S3). The definitions of the method detection limits
174 (MDLs) are described in Text S3, and the derived MDLs are given in Table S4. The
175 breakthrough of PUF plugs was checked in eleven split PUFs, and the results show
176 that the individual OPs in the second half varied from 8% to 23% (Table S5),
177 indicating good retention capacity. Certified surrogate standards (from Dr.
178 Ehrenstorfer GmbH, Germany) were added to each sample before extraction and
179 analysis. The recoveries ranged from 71% to 94% for PCB 30, 79% to 105% for
180 Mirex, and 65% to 92% for perylene-D12. The reported concentrations were
181 subtracted by mean blanks but not corrected for recoveries. To check the
182 reproducibility of the chiral analysis, the racemic standard of α -HCH was injected
183 repeatedly and its average EF value was 0.499 ± 0.001 ($n = 5$).

184 **2.5 Calculations of air-water gas exchange**

185 Concurrent air and water samples were used to assess the status of air-water gas
186 exchange in Nam Co Lake. The gas exchange direction can be determined by the ratio
187 of fugacity in water (f_w) and air (f_a), giving the fugacity ratio (f_w/f_a) (Jantunen et al.,

188 2015):

$$189 \quad f_a = C_G R T_a \quad (1)$$

$$190 \quad f_w = C_w H \quad (2)$$

191 where C_G and C_w are the gaseous and dissolved concentrations of target compounds in
192 air and water (mol m^{-3}), respectively, R is the gas constant ($8.314 \text{ Pa m}^3 \text{ mol}^{-1} \text{ K}^{-1}$), T_a
193 (K) is the air temperature, and H ($\text{Pa m}^3 \text{ mol}^{-1}$) is the Henry's law constant. Due to the
194 possible sorption by dissolved organic carbon (DOC), OPs retained by XAD were
195 DOC-corrected to derive the truly freely dissolved concentrations in water (Text S4)
196 (Gonzalez-Gaya et al., 2016). H values were adjusted for the real water temperature
197 and salinity of Nam Co by the procedure described in Text S5 (Cetin et al., 2006; Ma
198 et al., 2010). The uncertainty involved in f_w/f_a was estimated by propagating the errors
199 in C_a (30%), C_w (35%), and H (20%), which was 50%. Accordingly, ratios of f_w/f_a
200 between 0.5 and 1.5 are assumed as air-water equilibrium, while $f_w/f_a > 1.5$ and < 0.5
201 indicate net volatilization and deposition, respectively.

202 Net fluxes of air-water gas exchange (F_{AW} , $\text{ng m}^{-2} \text{ day}^{-1}$) were quantified using the
203 Whitman two-film model, which has been used in many previous studies (Iwata et al.,
204 1993; Khairy et al., 2014):

$$205 \quad F_{AW} = K_{ol} (C_w - C_G R T_a / H) \quad (3)$$

206 where K_{ol} (m s^{-1}) is the overall mass transfer coefficient, which contains contributions
207 from the mass transfer coefficients of the water and air layers, K_w and K_a , respectively.
208 They are related to the wind speed and compound-specific molecular diffusivity; a
209 detailed calculation is presented in Text S6. Positive flux values indicate net
210 volatilization, and negative values indicate net deposition.

211 **2.6 Estimation of dry and wet deposition fluxes**

212 In addition to the gas exchange, dry and wet deposition are also important processes
213 that control the input of OPs from air to lake. Dry deposition fluxes (F_{DD} , $\text{ng m}^{-2} \text{ day}^{-1}$)
214 of atmospheric particulate-phase OPs can be calculated using (Gonzalez-Gaya et al.,
215 2016) the following equation:

216
$$F_{DD}=0.864V_D C_P \quad (4)$$

217 where V_D (cm s^{-1}) is the compound specific deposition velocity, C_P is the measured
218 OPs concentrations in TSP (pg m^{-3}), and 0.864 is a unit conversion factor. V_D for each
219 sampling period and compound was estimated using an empirical equation derived by
220 Gonzalez-Gaya et al. (2014):

221
$$\log(V_D)=-0.261\log(P_L)+0.387U_{10}Chl_s-3.082 \quad (5)$$

222 where P_L (Pa) is subcooled liquid vapor pressure of chemicals that was corrected to
223 the local temperature using the equations given in Table S6, U_{10} (m s^{-1}) is wind speed
224 at 10 m height converted from the field-measured wind speed at 1.5 m (Table S1), and
225 Chl_s is the surface chlorophyll concentration (mg m^{-3} , Liu et al., 2010).

226 Wet deposition fluxes by rain (F_{WD} , $\text{ng m}^{-2} \text{day}^{-1}$) were estimated using the method
227 established by Jurado et al. (2005):

228
$$F_{WD}=P(W_G C_G + W_P C_P) \quad (6)$$

229 where P is precipitation depth per day (m d^{-1}) derived from the data recorded in the
230 NCMORS, and W_G and W_P are the gas and particle washout ratios, respectively.
231 Assuming that equilibrium is attained between the gas phase and the dissolved phase
232 in a raindrop, W_G was estimated by (Wania et al., 1998a):

233
$$W_G=RT_a/H \quad (7)$$

234 The recommended value of W_P in Jurado et al. (2005) was used to consider the
235 particle scavenging by rain.

236 For snow deposition, the fluxes were calculated by adopting the washout ratios
237 reported in Franz and Eisenreich (1998) (Table S7).

238 **3. Results and discussion**

239 We determined the OP concentrations in air, TSP, water, and SPM separately; the full
240 data sets are listed in Tables S8-S11. OCPs and PCBs were rarely detected in TSP
241 (Table S9), and were therefore not considered in further discussion. Comparisons
242 between the data from this study and previously published values for the TP and other
243 remote regions are presented in Tables S12-S15.

244 3.1 Levels of OPs in air and water at Nam Co

245 The concentrations of OPs in the atmosphere and TSP in Nam Co are summarized in
246 Figure 2 using box-and-whisker plots. Among the OCPs, HCB was the dominant
247 chemical with an average concentration of 20 pg m^{-3} (Figure 2a), which was two
248 times higher than that reported for southeastern TP (Sheng et al., 2013) and Mt.
249 Everest (Li et al., 2006) (Table S12), but lower than the values in the Rocky
250 Mountains (42 pg m^{-3} , Wilkinson et al., 2005) and the Arctic (64 pg m^{-3} , Su et al.,
251 2006). The α -HCH (average 4.0 pg m^{-3}) and γ -HCH (2.1 pg m^{-3}) values in this study
252 were much lower than those measured using a flow-through sampler (FTS) during
253 2006 to 2008 (48.7 and 7.9 pg m^{-3} , respectively) (Xiao et al., 2010). The DDT
254 concentrations in the current study (0.8 - 46.4 pg m^{-3}) were lower than those observed
255 for Lulang in southeastern TP (Table S12) (Sheng et al., 2013), which is the entrance
256 of the Indian Monsoon. In spite of this, the levels of DDTs were still one order of
257 magnitude higher than those for the Arctic (Table S12) (Su et al., 2008). Lower
258 concentrations of $\sum_6\text{PCBs}$ were also detected in air with an average value of 2.5 pg
259 m^{-3} .

260 The sum concentrations of $\sum_{15}\text{PAHs}$ in the atmosphere ranged from 0.5 – 13 and
261 0.1 – 3.4 ng m^{-3} in the gaseous and particulate phases, with averages of 2.2 and 0.6 ng
262 m^{-3} , respectively. The 3- and 4-ring PAHs were predominant in both phases, including
263 Phe, Flu, Fla, and Pyr (Figure 2b and 2c). The PAH levels in Nam Co were one order
264 of magnitude lower than those reported for Lhasa (35.7 ng m^{-3} , Table S13), which is
265 the capital city of Tibet with a large population, extensive tourism, and abundant
266 religious activities (Gong et al., 2011). Compared with background levels in other
267 regions of the world (Table S13), the PAHs in this study were comparable to the
268 levels in Arctic air (Ding et al., 2007), but significantly higher than those from
269 European mountainous regions (Fernandez et al., 2002).

270 In the lake water, the average dissolved concentrations of α -HCH, β -HCH, γ -HCH,
271 HCB, and PCB 28 were 9.9 , 85.2 , 7.0 , 7.6 , and 1.9 pg L^{-1} , respectively; while
272 DDT-related compounds were below MDLs in most cases for both dissolved and

273 SPM phases (Table S10 and S11). The current measured HCH concentrations were
274 approximately two orders of magnitude lower than values reported for the Yamdrok
275 and Co Ngoin Lake in 2002 (Table S14) (Zhang et al., 2003). Two possible reasons
276 for this discrepancy are: i) the inter-annual variation of chemicals, i.e., the
277 concentrations declined rapidly since 2002; and ii) the uncertainties caused by
278 analytical and instrumental method (electron capture detector in Zhang et al. (2003)
279 study and the MS detector in the current study). From a global perspective, the HCH
280 concentrations obtained by this study were overall lower than those in European
281 mountain lakes (Table S14). DDT class chemicals were rarely detected and only PCB
282 28 could be quantified in the Nam Co lake water. These features combined with the
283 low levels of HCHs suggest that the OP levels in Nam Co lake water were close to the
284 values reported for ocean waters, such as, the North Atlantic and Arctic oceans (with
285 DDTs and PCBs mostly below the detection level, or $<1 \text{ pg L}^{-1}$) (Gioia et al., 2008;
286 Lohmann et al., 2009). By contrast, high levels of PAHs were found in the Nam Co
287 lake water, ranging from 6.9 to 83.6 and 1.7 to 28 ng L^{-1} for the dissolved and SPM
288 phases, respectively. The dissolved $\sum_{15}\text{PAH}$ levels were one order of magnitude
289 higher than those reported for Himalayan high-altitude lakes in Nepal (Table S15)
290 (Guzzella et al., 2011) and the Great Lakes (Table S15) (Venier et al., 2014), and two
291 orders of magnitude greater than values for open oceans (Table S15) (Ma et al., 2013)
292 and European mountain lakes (Table S15) (Vilanova et al., 2001).

293 **3.2 Possible sources**

294 Long range atmospheric transport (LRAT) is considered an important source
295 contributing to the occurrence of OPs in remote environments (Dalla Valle et al.,
296 2005). Considering that the prevailing climate system operating over Nam Co in
297 summer is the Indian Monsoon, if the seasonal pattern of a chemical is similar to that
298 of the monsoon, monsoon transport may therefore be the source of OPs in Nam Co air.
299 Thus, the interrelationship between monsoon intensity (Indian Monsoon Index, IMI,
300 W m^{-2}) and OP concentrations was investigated (Figure 3). Figure 3 shows that
301 α -HCH and *o,p'*-DDT displayed synchronous seasonal variation with the IMI. This

302 suggests that monsoon transport was the principal reason for the occurrence of OCPs
303 in the Nam Co atmosphere. In addition, isomer ratios can provide insight on the
304 source and fate of the OPs. In this study, we found that the isomer ratios of *p,p'*-DDT
305 to *p,p'*-DDE were broadly in agreement with those found for the source regions of
306 India and the Bay of Bengal (Table S16) (Gioia et al., 2012; Zhang et al., 2008).
307 Similar to other remote regions, such as, the Arctic (Hung et al., 2010), Antarctic
308 (Baek et al., 2011), Rocky Mountains (Daly et al., 2007), and southeastern TP (Sheng
309 et al., 2013), in which LRAT is the primary transport mode of OPs, the dominance of
310 α - to γ -HCH was observed in the Nam Co atmosphere (Table S16). Results of isomer
311 ratios associated with the seasonal variations supported the interpretation that OCPs in
312 the Nam Co atmosphere had undergone LRAT. In contrast to OCPs, neither the
313 gaseous nor the particulate phases of PAHs showed a clear and consistent seasonal
314 variation during the two years of air monitoring (Figure S3), which is likely because
315 there were primary emissions of PAHs surrounding the Nam Co region.

316 Apart from the seasonal trends, spatial distribution patterns can also provide valuable
317 information on OP sources. The spatial distributions of OPs in the surface water
318 across the Nam Co Lake are presented in Figure 4. First, HCHs showed a uniform
319 distribution (Figure 4) without significant differences among the different regions of
320 the lake (Table S17). The even distribution of HCHs in the water was most likely
321 caused by the LRAT origins and relatively higher water solubility. Second, relatively
322 high levels of HCB and PAHs occurred in water from the northwestern and eastern
323 parts of the lake (Table S17 and Figure 4). The elevated HCB and PAHs in these
324 regions were likely related to anthropogenic activity in the vicinity. As shown in
325 Figure 1b, two townships (Baoji and Namco), which have the highest population
326 around Nam Co Lake, are located in the northwestern and eastern corners of the lake.
327 Following a traditional lifestyle, the residents use large amounts of local biomass
328 (mostly yak dung) for cooking and heating (Xiao et al., 2015). High PAH
329 concentrations have been reported in local Tibetan tents that were emitted mainly
330 from burning yak dung (Li et al., 2012). A ratio of $BaA/(BaA+Chr) = 0.33$ was

331 recommended as a specific diagnostic fingerprint for yak dung combustion (Li et al.,
332 2012). The BaA/(BaA+Chr) ratios observed in our study (0.27 ± 0.08 for air and
333 0.24 ± 0.10 for water) were in good agreement with this diagnostic ratio. This suggests
334 that local combustion emission is likely the source of PAHs in Nam Co. With the
335 exception of PAHs, biomass combustion can also produce HCB (Bailey, 2001), which
336 may be the reason for the higher HCB concentrations occurring around the townships.
337 The spatial distribution of OPs in the Nam Co lake water highlights the important
338 contribution of local sources for PAHs and HCB.

339 **3.3 LRAT versus re-volatilization**

340 From the above results, we found that LRAT is a key factor that determines the
341 seasonality of the atmospheric HCHs and DDTs in Nam Co (higher concentrations
342 occurred in summer). However, high temperatures generally occur during summer,
343 which may promote the evaporation of chemicals from local surfaces (e.g., soils and
344 water bodies). To what extent does this re-evaporation contribute to the atmospheric
345 OPs? The Clausius-Clapeyron (C.C.) equation can be used to assess this probability
346 (Wania et al., 1998b). If a strong relationship is found between the partial pressure of
347 atmospheric OCPs and the air temperature, this indicates that volatilization may occur.
348 Otherwise, low temperature dependence will occur in the case of LRAT. In the
349 present study, the results of the C.C. equation are summarized in Table S18. The
350 correlation with temperature ($p > 0.05$, Table S18) for most chemicals was not
351 significant, except for α -HCH, which displayed a relatively lower correlation
352 coefficient ($R^2 = 0.29$, $p < 0.05$, Table S18). This indicates that weak volatilization of
353 α -HCH from local surfaces at Nam Co may exist, while the re-evaporation of other
354 chemicals is limited.

355 Enantiomers of chiral OPs have been used to distinguish the contribution of LRAT
356 and re-volatilization of OPs from surfaces (Bidleman et al., 2012). For example,
357 technical HCH contains the (+)- and (-)- α -HCH enantiomers in a racemic proportion
358 (EF=0.5). Abiotic processes (transport, hydrolysis, and photolysis) do not favor either
359 enantiomer, while only biological processes, such as, microbial degradation in soils

360 and water, show enantioselectivity and will alter the EFs of α -HCH (Ridal et al.,
361 1997). Therefore, nearly racemic signatures usually indicate input from LRAT, while
362 nonracemic signatures represent the influence of local microbial degradation. In the
363 present study, both the enantiomeric signatures of α -HCH in air and water were
364 measured simultaneously from May to September. As shown in Figure 5a, all the lake
365 water samples showed a selective depletion of (+)- α -HCH, with EFs ranging from
366 0.318 to 0.449. This has previously been reported for other cold oligotrophic water
367 systems, such as the Arctic lakes (EFs: 0.359–0.432) (Law et al., 2001). From Figure
368 5a, we found that extensive enantioselective degradation occurred in June and July,
369 which coincided with the bacterial bloom period (Figure 5b) (Liu et al., 2013). This
370 negative correlation between the EF of α -HCH in lake water and bacterial abundance
371 is presented in Figure S4. Law et al. (2001) suggested that under low nutrient
372 conditions, oligotrophic bacteria are able to use xenobiotic carbon sources, such as
373 α -HCH. This implies that the Tibetan lake microbes can also metabolize, or
374 cometabolize, α -HCH.

375 If high temperatures favor the evaporation of α -HCH from the lake water, depletion of
376 (+)- α -HCH should be observed for air. However, the EFs of the air samples were
377 overall racemic. This is similar to the racemic composition observed in the
378 atmosphere over Indian regions (Huang et al., 2013), which is the potential source
379 region of HCHs in Nam Co. With respect to the enantiomeric signature in air samples
380 from June and July, only some (+) α -HCH depletion was observed in air (Figure 5a),
381 indicating weak evaporation of α -HCH from the lake water. Combined with the EF
382 values in air and water, the fraction of the contribution from lake water volatilization
383 (f) can be quantified by (Huang et al., 2013):

$$384 \quad f = (EF_a - EF_b) / (EF_w - EF_b) \quad (8)$$

385 where EF_a and EF_w are the EF values in air and water, respectively; and EF_b is the
386 background EF value in air, which was assumed to be the average EF of the standard.
387 The estimated results show that only 19% and 17% of atmospheric α -HCH came from
388 water volatilization in June and July, respectively, demonstrating that LRAT is indeed

389 the major source (more than 80%) of α -HCH. This result is in contrast with the
390 conclusion of Xiao et al. (2010) that evaporation from Nam Co Lake largely
391 contributed to the atmospheric α -HCH concentration. In that study, both levels and
392 enantiomeric signatures of α -HCH in Nam Co lake water were absent.

393 **3.4 Atmospheric processes**

394 **3.4.1 Air-water gas exchange**

395 Although some α -HCH evaporation was recorded in June and July, the air-water
396 exchange process during the entire ablation period is of great concern as this is the
397 main season transferring pollutants between air and water. Fugacity ratios (f_w/f_a) and
398 net exchange fluxes (F_{AW} , $\text{ng m}^{-2} \text{ day}^{-1}$) were quantified using paired air-water
399 samples collected from May to September in 2014. The average exchange status
400 (average of f_w/f_a) for HCHs, HCB, PCB 28, and PAHs during the ablation period is
401 illustrated in Figure 6. Because of DDTs, Ant and Fla were not quantified in the lake
402 water (Table S10) and were therefore excluded from the discussion. α - and γ -HCH
403 had low f_w/f_a values ranging from 0.08 to 0.15, and 0.02 to 0.08, respectively (Figure
404 6a). The low f_w/f_a ratio suggests that α - and γ -HCH were overall prone to deposition
405 from air to water during the ablation period. The deposition fluxes were $-1.6 \pm 0.4 \text{ ng}$
406 $\text{m}^{-2} \text{ day}^{-1}$ for α -HCH and $-1.0 \pm 0.2 \text{ ng m}^{-2} \text{ day}^{-1}$ for γ -HCH, which are within the
407 same order of magnitude as those reported for the Great Lakes (Khairy et al., 2014).
408 Connected to the source of HCHs discussed above, this result implies that the
409 following LRAT-deposition event of HCHs occurred in the ablation period of Nam Co
410 Lake. In terms of β -HCH, HCB, and PCB 28, their f_w/f_a ratios were either overlapping
411 with the equilibrium range (0.5-1.5) or on the edge of deposition threshold. Therefore,
412 low deposition fluxes for β -HCH ($-0.2 \text{ ng m}^{-2} \text{ day}^{-1}$) and PCB 28 ($-0.1 \text{ ng m}^{-2} \text{ day}^{-1}$),
413 and large variability for HCB ($-1.0 \pm 0.6 \text{ ng m}^{-2} \text{ day}^{-1}$) were observed (Figure 7a).

414 The results of the air-water gas exchange for PAHs are presented in Figure 6b. The
415 fugacity ratios of thirteen PAHs varied depending on their molecular weight and
416 volatility (Figure 6b). Acel, Ace, and Flu showed f_w/f_a values significantly higher than
417 1.5 (Figure 6b), indicating that the lake acted as a secondary source for these volatile

418 chemicals. The f_w/f_a values for Phe covered a large range (from 0.3 to 3), showing a
419 shift between volatilization and deposition (Figure 6b). Other high molecular weight
420 (MW > 202) PAHs, including Pyr, BaA, Chr, Bbf, Bkf, Bap, IcdP, DahA, and BghiP,
421 favored net deposition with f_w/f_a values lower than 0.5 (Figure 6b). Greater
422 volatilization fluxes were observed for Acel, Ace, and Flu (3-ring), which could reach
423 up to 203 ng m⁻² day⁻¹ (Figure 7b). Whereas, the gaseous deposition fluxes for high
424 molecular weight PAHs were two orders of magnitudes lower and only varied from
425 -1.0 to -4.6 ng m⁻² day⁻¹ (Figure 7c). Although average deposition fluxes of 339 ng
426 m⁻² day⁻¹ were calculated for Phe, the deposition fluxes showed large variability (± 604
427 ng m⁻² day⁻¹). This result is broadly consistent with the exchange direction revealed by
428 the f_w/f_a values, implying that the exchange of Phe between air and water may be
429 reversed during the entire ablation period.

430 **3.4.2 Reversal of the air-water exchange of Phe**

431 In section 3.4.1, we observed that both the air-water exchange direction and the flux
432 of Phe showed a large range of values and uncertainties. This raises a question about
433 what drives this variation. The monthly calculated f_w/f_a and F_{AW} of Phe during the
434 ablation period showed that the volatilization of Phe occurred during May and June,
435 but deposition begun in July, which represents a reversal (Figure 8). Given that lake
436 ice begins melting during May, the melted ice may discharge large amounts of
437 accumulated PAHs into the lake, causing the relative enrichment (high fugacity) of
438 Phe in the water, and triggering the secondary emission of Phe from the water to the
439 atmosphere. This was confirmed by the increased water concentration of Phe found
440 during May and June (Table S10). This is also the reason why a large uncertainty of
441 F_{AW} was observed for Phe during the ablation period. Linked to the source of PAHs
442 discussed above, the final exchange status of PAHs is the combined effects of the
443 depositional input caused by biomass burning, the properties of the chemical, and the
444 melting of lake ice.

445 Seasonal ice cover is an important feature of water bodies in cold regions. In the
446 Arctic region, Jantunen et al. (2008) and Wong et al. (2011) both observed the

447 occurrence of volatilization of OCPs from seawater coincident with the breaking up of
448 ice cover in the summer. The Nam Co Lake also undergoes long periods of ice-cover
449 (Liu et al., 2013). During the winter, the lake surface is covered by ice and gas
450 exchange is restricted, meanwhile dry and wet deposition exerts a significant
451 influence on the input inventory of PAHs to the lake. Both of these two deposition
452 processes are one-way (no volatilization), which keeps the contaminants being
453 accumulated. As summer arrives, the lake ice begins to thaw and air-water gas
454 exchange begins to dominate. On the one hand, after the higher accumulation of
455 deposition, supersaturation of PAHs in the lake may occur. On the other hand, the
456 fugacity capacity of ice is much higher than that of water, and therefore the decrease
457 of the fugacity capacity during melting will increase the fugacity of the PAHs (Wania
458 et al., 1998c), which also promotes their re-emission from the water. Although the
459 seasonal ice cover did not show any obvious influence on the fate of OCPs and other
460 PAHs, it played an important role in the fate of Phe, which was a dominant compound
461 in the Nam Co atmosphere. The lake therefore acted as a secondary source of Phe in
462 May and June, and shifted to a net sink during other months, which is likely driven by
463 the seasonal freeze-thaw cycle of lake ice (Figure 8).

464 **3.4.3 Atmospheric degradation**

465 Reactions with the hydroxyl radical (OH) are an important removal process of
466 gaseous OPs from the atmosphere. The resulting degradation fluxes (F_{deg} , $\text{ng m}^{-2} \text{ day}^{-1}$)
467 are dependent on the concentration of OH radicals in the air (Spivakovsky et al., 2000)
468 and the compound-specific degradation rate constant (K_{OH} , $\text{cm}^3 \text{ molecules}^{-1} \text{ day}^{-1}$).
469 The K_{OH} values of gaseous OCPs and PAHs are from Brubaker and Hites (1998) and
470 Keyte et al. (2013), respectively. Due to the lack of information on K_{OH} for β -HCH
471 and BaA, their degradation fluxes (F_{deg}) were not considered in this study. The
472 calculated F_{deg} values were averaged for individual OPs and are presented in Figure
473 S5. The degradation fluxes for α -, γ -HCH, HCB, and PCB 28 ranged between 0.3 and
474 $0.9 \text{ pg m}^{-2} \text{ day}^{-1}$ (Figure S5), 3 orders of magnitude lower than their F_{AW} . This
475 indicates that the contribution of atmospheric degradation to their total inventory in

476 the environment is negligible.

477 In contrast to the OCPs, the PAHs are more susceptible to photodegradation
478 (Lohmann et al., 2009). In our study, lower molecular weight PAHs showed higher
479 degradation fluxes, such as 4–184 ng m⁻² day⁻¹ for Phe, and 1–160 ng m⁻² day⁻¹ for
480 Ant (Figure S5). These values are similar to those reported for F_{deg} in the remote
481 atmosphere of the Atlantic Ocean (i.e., 7–120 and 9–50 ng m⁻² day⁻¹ for Phe and Ant,
482 respectively) (Nizzetto et al., 2008). We observed relatively low F_{deg} values for 5- and
483 6-ring PAHs, ranging from 0.01 to 0.18 ng m⁻² day⁻¹ (Figure S5). Generally, the F_{deg}
484 of all PAH compounds was one order of magnitude lower than their F_{AW} . OH
485 depletion is the primary process that removes atmospheric PAHs, presumably causing
486 the continuous volatilization of low molecular weight PAHs from the water. This
487 raised questions about other processes that may have supplied PAHs into the lake
488 water. On the other hand, OH degradation also decreases the input of high molecular
489 weight PAHs into the water and it is unclear to what extent this degradation
490 counteracts other deposition processes.

491 **3.4.4 Atmospheric deposition**

492 In addition to the gas exchange, dry and wet deposition are also important processes
493 that influence the input of OPs from air to the lake. Dry (F_{DD}) and wet (F_{WD})
494 deposition fluxes were estimated using the method described above (section 2.6).
495 With respect to HCHs, HCB, and PCB 28, their dry deposition fluxes (F_{DD}) were
496 negligible due to their low detection frequency in the particulate phase (Table S9).
497 However, the average F_{WD} for α -HCH, β -HCH, and γ -HCH was -0.3, -0.9, and -0.4 ng
498 m⁻² day⁻¹, respectively, which is comparable to their F_{AW} levels. F_{WD} for HCB (-0.02
499 ng m⁻² day⁻¹) and PCB 28 (-0.002 ng m⁻² day⁻¹) was two magnitudes lower than their
500 F_{AW} . In general, precipitation scavenging is most efficient in HCHs compared with
501 the other chemicals (Carrera et al., 2002). Greater wet deposition fluxes of HCHs
502 occurred in August (Figure S6), coinciding with the highest amount of precipitation in
503 Nam Co. Combining the F_{AW} and F_{WD} of HCHs, the estimated annual input of HCHs
504 from air into the whole lake (2015 km²) was 1.9 kg year⁻¹. This result highlights the

505 input of HCHs by the LRAT-deposition process during the ablation period (open
506 water season). Snow scavenging of HCHs has been reported as an important clearing
507 process in mountain regions (Kang et al., 2009). However, the transport of HCHs in
508 winter is very limited due to the unfavorable air circulation patterns (westerly wind),
509 ruling out the significant contribution of input of HCHs by snow scavenging.

510 Compared with OCPs, the close association between PAHs and the particulate phase
511 accounted for their relatively higher deposition fluxes. The estimated dry and wet
512 deposition fluxes for individual PAHs during the ablation and frozen periods,
513 respectively, are provided in Table 1. We found that the F_{DD} values of PAHs for the
514 ablation period are, in general, lower than those for the frozen period. For example,
515 the F_{DD} of total $\sum_{15}PAHs$ increased by one order of magnitude from the ablation
516 period ($4.5 \text{ ng m}^{-2} \text{ day}^{-1}$) to the frozen period ($38 \text{ ng m}^{-2} \text{ day}^{-1}$; Table 1). Two factors
517 may lead to the increase of F_{DD} in winter: the increased wind speed during the winter
518 season and the growing particulate-PAH concentrations due to the enhanced
519 combustion activities in winter. Compared with other studies, the estimated F_{DD} for
520 the total $\sum_{15}PAHs$ ($4.5\text{--}38 \text{ ng m}^{-2} \text{ day}^{-1}$, this study) is broadly within the range
521 reported for global oceans ($8.3\text{--}52.4 \text{ ng m}^{-2} \text{ day}^{-1}$) (Gonzalez-Gaya et al., 2014).

522 Wet deposition was found to be the dominant deposition process for the input of PAHs
523 into Nam Co (Table 1). This was expected because precipitation scavenging of
524 organic chemicals underlies the accumulation of pollutants in mountain regions
525 (Tremolada et al., 2008). In addition, there was an obvious difference between the
526 values of F_{WD} during the ablation and frozen periods. For the total 15 PAHs, the F_{WD}
527 in the frozen period ($702 \text{ ng m}^{-2} \text{ day}^{-1}$) was approximately 5 times higher than that for
528 the ablation period ($161 \text{ ng m}^{-2} \text{ day}^{-1}$), which may be due to the different precipitation
529 types between these two periods (snow vs. rain). Snow has been suggested to be more
530 efficient than rain for scavenging particulate-PAHs, which had a high concentration
531 during winter in Nam Co (Table S9). Thus, although the precipitation of Nam Co in
532 winter is low (less than 30 mm, Figure S2), the strong scavenging ratio of snow to
533 PAHs combined with the relatively high particulate-PAHs concentration in winter

534 caused the enhanced PAHs deposition in winter. The frozen season coincided with the
535 period of high emission and high deposition of PAHs, implying a significant
536 contribution of this season in the input of PAHs into the lake.

537 To calculate the comprehensive contribution of all above-mentioned processes, three
538 groups of PAHs were classified in Table 1 based on their fate during the air-water
539 exchange processes. PAHs (Acel, Ace, and Flu) showing volatilization behavior were
540 placed into one group, PAHs with large F_{AW} variability between the status of
541 volatilization and deposition were in the second group; and the remaining PAHs
542 displaying deposition behavior were placed into the third group (Table 1). In this
543 classification, although the air-water exchange direction and fluxes of Ant and Fla
544 cannot be estimated, we still placed them into the second group because of their
545 similarity to Phe in their physicochemical properties. For the volatilization group, the
546 total outgassing from the lake was estimated to be approximately 126 kg per year,
547 which cannot alone be supplied by their total deposition flux (sum of F_{WD} and F_{DD}).
548 This suggests that there may be additional natural sources of PAHs in the lake, such as,
549 degradation of pigments carrying aromatic structure and turnover of organic matter
550 (Nizzetto et al., 2008). Regarding the deposition group (Pyr, BaA, Chr, Bbf, Bkf, Bap,
551 IcdP, DahA, and BghiP), their total deposition flux ($F_{AW}+F_{DD}+F_{WD}$) will roughly
552 cause the annual input of 208 kg high molecular weight PAHs into the lake. Although
553 the F_{AW} of Phe was reversed and the total volatilization of Phe was estimated at
554 around 26 kg year⁻¹, this loss will be complemented by the continuous deposition of
555 Phe (~373 kg year⁻¹) from July to April. This indicates that the annual net input of Phe
556 will be above 340 kg, which suggests that Phe is the most dominant contributor in the
557 total PAHs deposition. In addition to the 15 PAHs considered here, there are other
558 PAHs with high abundances, for example alkylated phenanthrenes, which will drive a
559 much larger depositional fluxes to the lake.

560 **3.4.5 Uncertainties in flux estimation**

561 Several factors were involved in the uncertainties of the flux estimation: (i) loss
562 during sample extraction and clean-up; (ii) measurement errors; and (iii) accuracy of

563 the parameters in meteorology and physicochemical properties. The air-water gas
564 exchange flux (F_{AW}) is the most important contributor to the total inventory of PAHs
565 into the lake. The uncertainty involved in F_{AW} was estimated by propagating the
566 errors in C_a (30%), C_w (35%), K_{ol} (40%), and H (20%), which was 64%. This small
567 error demonstrates that the estimate of the gas exchange fluxes was relatively robust.
568 By contrast, the uncertainties in other fluxes were higher. The uncertainty of F_{DD} was
569 estimated as a factor of 3 (Gonzalez-Gaya et al., 2014). However, the uncertainties of
570 F_{deg} and F_{WD} are difficult to quantify due to unavailable data on the relative errors of
571 K_{OH} , W_G , and W_P . For example, the scavenging rates of PAHs by wet deposition were
572 highly variable, which was caused by the complexity of the size distribution of
573 aerosols, meteorological conditions, and the scavenging process (Jurado et al., 2005).
574 Considering these aggregated uncertainties, the estimated total fluxes here are only
575 expected to capture the order of magnitude for the different processes. In addition,
576 other input processes into the lake, such as, glacier meltwater, river runoff, and soil
577 erosion may also occur in this study region, which will lead to an underestimation of
578 the total input flux.

579 **3.5 Implication for the regional carbon cycling**

580 Lakes are increasingly recognized as an important component of the terrestrial carbon
581 cycle (Tranvik et al., 2009). Nearly 50% of the area of Chinese lakes is located on the
582 TP, with general oligotrophic conditions and a total lake area of $>43000 \text{ km}^2$ (Zhang
583 et al., 2014). Compared with other components, such as grassland and forest, organic
584 carbon burial in Tibetan lakes has been largely ignored. Although our study only
585 focused on one of these lakes (Nam Co, area = 2015 km^2), we can extrapolate the
586 annual atmospheric deposition of $\sum_{15}\text{PAHs}$ into the remaining Tibetan lakes, and
587 estimate it at 8.7 tonnes C, when expressed as carbon fluxes (Gonzalez-Gaya et al.,
588 2016). In addition to these 15 PAHs, there are other carbon sources such as soot, DOC,
589 PAHs derivatives, and other anthropogenic organic compounds, which would become
590 a significant allochthonous carbon source for the oligotrophic lakes in TP. Because the
591 Tibetan lakes are low in nutrients, bacteria in the lake have adapted to using a wide

592 range of organic compounds and growing under starvation conditions (Liu et al.,
593 2009). Recently, bacteria from the genus *Sphingomonas* were detected in Nam Co
594 lake water and various glacier snows of the TP (Liu et al., 2013; Liu et al., 2009), and
595 they were reported to have the ability to degrade PAHs (Leys et al., 2005). The
596 presence of these bacteria in Nam Co suggests that the atmospheric inputs of organic
597 pollutants can act as a carbon source to support the survival of Tibetan microbial
598 communities. Despite the natural PAH background in the environment, increasing
599 biomass burning has led to the accumulation of PAHs in the lake sediments,
600 especially during the past 50 years (Yang et al., 2016). Therefore, the continuous
601 atmospheric deposition of various PAHs and their ecological impact deserve greater
602 concern.

603 **4. Conclusions**

604 This study confirmed that the Nam Co Lake was still a net sink of HCHs, following
605 the LRAT-deposition process, rather than a secondary source. By contrast, PAHs
606 primarily originated from local biomass burning. Dominated by gas exchange and wet
607 deposition, the air-water fluxes of $\sum_{15}\text{PAHs}$ to the whole Nam Co Lake were
608 estimated to be 550 kg year^{-1} , providing a substantial carbon source for the
609 oligotrophic lake. Among the PAHs compounds, Phe showed a distinct behavior with
610 monthly reversals of the air–water exchange, which was most likely driven by the
611 seasonal melting of lake ice. This hypothesis requires further investigation, and a
612 passive sampling technique is recommended as a viable alternative to enhance the
613 spatial coverage of the investigation of air-water exchange in the TP.

614 **Acknowledgments**

615 This study was supported by the National Natural Science Foundation of China
616 (41671480, 41222010 and 41571463) and Youth Innovation Promotion Association
617 (CAS2011067). The authors would like to thank the staff at Nam Co Monitoring and
618 Research Station for Multisphere Interactions for their help with the field sampling.

619 **References:**

- 620 Baek, S. Y., Choi, S. D., and Chang, Y. S.: Three-Year Atmospheric Monitoring of Organochlorine
621 Pesticides and Polychlorinated Biphenyls in Polar Regions and the South Pacific, *Environ.*
622 *Sci. Technol.*, 45, 4475-4482, doi: 10.1021/Es1042996, 2011.
- 623 Bailey, R. E.: Global hexachlorobenzene emissions, *Chemosphere*, 43, 167-182, doi:Doi
624 10.1016/S0045-6535(00)00186-7, 2001.
- 625 Bidleman, T. F., Jantunen, L. M., Kurt-Karakus, P. B., and Wong, F.: Chiral persistent organic
626 pollutants as tracers of atmospheric sources and fate: review and prospects for investigating
627 climate change influences, *Atmospheric Pollution Research*, 3, 371-382, doi:
628 10.5094/Apr.2012.043, 2012.
- 629 Brubaker, W. W., and Hites, R. A.: OH Reaction Kinetics of Gas-Phase α - and
630 γ -Hexachlorocyclohexane and Hexachlorobenzene, *Environ. Sci. Technol.*, 32, 766-769,
631 1998.
- 632 Carrera, G., Fernández, P., Grimalt, J. O., Ventura, M., Camarero, L., Catalan, J., Nickus, U., Thies,
633 H., and Psenner, R.: Atmospheric deposition of organochlorine compounds to remote high
634 mountain lakes of Europe, *Environ. Sci. Technol.*, 36, 2581-2588, 2002.
- 635 Cetin, B., Ozer, S., Sofuoglu, A., and Odabasi, M.: Determination of Henry's law constants of
636 organochlorine pesticides in deionized and saline water as a function of temperature, *Atmos.*
637 *Environ.*, 40, 4538-4546, doi: 10.1016/j.atmosenv.2006.04.009, 2006.
- 638 Chakraborty, P., Zhang, G., Li, J., Sivakumar, A., and Jones, K. C.: Occurrence and sources of
639 selected organochlorine pesticides in the soil of seven major Indian cities: Assessment of
640 air-soil exchange, *Environ. Pollut.*, 204, 74-80, 2015.
- 641 Dalla Valle, M., Jurado, E., Dachs, J., Sweetman, A. J., and Jones, K. C.: The maximum reservoir
642 capacity of soils for persistent organic pollutants: implications for global cycling, *Environ.*
643 *Pollut.*, 134, 153-164, doi: 10.1016/j.envpol.2004.07.011, 2005.
- 644 Daly, G. L., Lei, Y. D., Teixeira, C., Muir, D. C. G., and Wania, F.: Pesticides in western Canadian
645 mountain air and soil, *Environ. Sci. Technol.*, 41, 6020-6025, doi: 10.1021/Es070848o, 2007.
- 646 Ding, X., Wang, X. M., Xie, Z. Q., Xiang, C. H., Mai, B. X., Sun, L. G., Zheng, M., Sheng, G. Y.,
647 Fu, J. M., and Poschl, U.: Atmospheric polycyclic aromatic hydrocarbons observed over the
648 North Pacific Ocean and the Arctic area: Spatial distribution and source identification, *Atmos.*
649 *Environ.*, 41, 2061-2072, doi:10.1016/j.atmosenv.2006.11.002, 2007.
- 650 Fernandez, P., Grimalt, J. O., and Vilanova, R. M.: Atmospheric gas-particle partitioning of
651 polycyclic aromatic hydrocarbons in high mountain regions of Europe, *Environ. Sci. Technol.*,
652 36, 1162-1168, doi: 10.1021/Es010190t, 2002.
- 653 Franz, T. P., and Eisenreich, S. J.: Snow scavenging of polychlorinated biphenyls and polycyclic
654 aromatic hydrocarbons in Minnesota, *Environ. Sci. Technol.*, 32, 1771-1778, doi:
655 10.1021/Es970601z, 1998.
- 656 Froescheis, O., Looser, R., Cailliet, G. M., Jarman, W. M., and Ballschmiter, K.: The deep-sea as a
657 final global sink of semivolatile persistent organic pollutants? Part I: PCBs in surface and
658 deep-sea dwelling fish of the North and South Atlantic and the Monterey Bay Canyon
659 (California), *Chemosphere*, 40, 651-660, doi: 10.1016/S0045-6535(99)00461-0, 2000.
- 660 Gioia, R., Lohmann, R., Dachs, J., Temme, C., Lakaschus, S., Schulz-Bull, D., Hand, I., and Jones,
661 K. C.: Polychlorinated biphenyls in air and water of the North Atlantic and Arctic Ocean, J.

662 Geophys. Res., 113, doi: 10.1029/2007jd009750, 2008.

663 Gioia, R., Li, J., Schuster, J., Zhang, Y. L., Zhang, G., Li, X. D., Spiro, B., Bhatia, R. S., Dachs, J.,
664 and Jones, K. C.: Factors Affecting the Occurrence and Transport of Atmospheric
665 Organochlorines in the China Sea and the Northern Indian and South East Atlantic Oceans,
666 Environ. Sci. Technol., 46, 10012-10021, doi: 10.1021/Es302037t, 2012.

667 Gong, P., Wang, X. P., and Yao, T. D.: Ambient distribution of particulate- and gas-phase n-alkanes
668 and polycyclic aromatic hydrocarbons in the Tibetan Plateau, Environmental Earth Sciences,
669 64, 1703-1711, doi:10.1007/s12665-011-0974-3, 2011.

670 Gonzalez-Gaya, B., Zuniga-Rival, J., Ojeda, M. J., Jimenez, B., and Dachs, J.: Field
671 Measurements of the Atmospheric Dry Deposition Fluxes and Velocities of Polycyclic
672 Aromatic Hydrocarbons to the Global Oceans, Environ. Sci. Technol., 48, 5583-5592,
673 doi:10.1021/es500846p, 2014.

674 Gonzalez-Gaya, B., Fernandez-Pinos, M. C., Morales, L., Mejanelle, L., Abad, E., Pina, B., Duarte,
675 C. M., Jimenez, B., and Dachs, J.: High atmosphere-ocean exchange of semivolatile aromatic
676 hydrocarbons, Nature Geoscience, 9, 438-442, doi:10.1038/NGEO2714, 2016.

677 Guglielmo, F., Stemmler, I., and Lammel, G.: The impact of organochlorines cycling in the
678 cryosphere on their global distribution and fate-1. Sea ice, Environ. Pollut., 162, 475-481,
679 doi:10.1016/j.envpol.2011.09.039, 2012.

680 Guzzella, L., Poma, G., De Paolis, A., Roscioli, C., and Viviano, G.: Organic persistent toxic
681 substances in soils, waters and sediments along an altitudinal gradient at Mt. Sagarmatha,
682 Himalayas, Nepal, Environ. Pollut., 159, 2552-2564, doi:10.1016/j.envpol.2011.06.015,
683 2011.

684 Geisz, H. N., Dickhut, R. M., Cochran, M. A., Fraser, W. R., and Ducklow, H. W.: Melting
685 glaciers: A probable source of DDT to the Antarctic marine ecosystem, Environ. Sci. Technol.,
686 42, 3958-3962, doi:10.1021/es702919n, 2008.

687 Harner, T., Wiberg, K., and Norstrom, R.: Enantiomer fractions are preferred to enantiomer ratios
688 for describing chiral signatures in environmental analysis, Environ. Sci. Technol., 34,
689 218-220, 2000.

690 Hu, T., Cao, J., Lee, S., Ho, K., Li, X., Liu, S., and Chen, J.: Physiochemical characteristics of
691 indoor PM_{2.5} with combustion of dried yak dung as biofuel in Tibetan Plateau, China, Indoor
692 & Built Environment, 191, 172-181, 2015.

693 Huang, Y. M., Xu, Y., Li, J., Xu, W. H., Zhang, G., Cheng, Z. N., Liu, J. W., Wang, Y., and Tian, C.
694 G.: Organochlorine Pesticides in the Atmosphere and Surface Water from the Equatorial
695 Indian Ocean: Enantiomeric Signatures, Sources, and Fate, Environ. Sci. Technol., 47,
696 13395-13403, doi: 10.1021/Es403138p, 2013.

697 Hung, H., Kallenborn, R., Breivik, K., Su, Y. S., Brorstrom-Lunden, E., Olafsdottir, K., Thorlacius,
698 J. M., Leppanen, S., Bossi, R., Skov, H., Mano, S., Patton, G. W., Stern, G., Sverko, E., and
699 Fellin, P.: Atmospheric monitoring of organic pollutants in the Arctic under the Arctic
700 Monitoring and Assessment Programme (AMAP): 1993-2006, Sci. Total Environ., 408,
701 2854-2873, doi: 10.1016/j.scitotenv.2009.10.044, 2010.

702 Iwata, H., Tanabe, S., Sakal, N., and Tatsukawa, R.: Distribution of Persistent Organochlorines in
703 the Oceanic Air and Surface Seawater and the Role of Ocean on Their Global Transport and
704 Fate, Environ. Sci. Technol., 27, 1080-1098, 1993.

705 Jantunen, L. M., Helm, P. A., Kylin, H., and Bidlemant, T. F.: Hexachlorocyclohexanes (HCHs) in

706 the Canadian archipelago. 2. Air-water gas exchange of alpha- and gamma-HCH, *Environ.*
707 *Sci. Technol.*, 42, 465-470, doi: 10.1021/Es071646v, 2008.

708 Jantunen, L. M., Wong, F., Gawor, A., Kylin, H., Helm, P. A., Stern, G. A., Strachan, W. M. J.,
709 Burniston, D. A., and Bidleman, T. F.: 20 Years of Air-Water Gas Exchange Observations for
710 Pesticides in the Western Arctic Ocean, *Environ. Sci. Technol.*, 49, 13844-13852,
711 doi:10.1021/acs.est.5b01303, 2015.

712 Jurado, E., Jaward, F., Lohmann, R., Jones, K. C., Simo, R., and Dachs, J.: Wet deposition of
713 persistent organic pollutants to the global oceans, *Environ. Sci. Technol.*, 39, 2426-2435, doi:
714 10.1021/Es048599g, 2005.

715 Kang, J. H., Choi, S. D., Park, H., Baek, S. Y., Hong, S., and Chang, Y. S.: Atmospheric deposition
716 of persistent organic pollutants to the East Rongbuk Glacier in the Himalayas, *Sci. Total*
717 *Environ.*, 408, 57-63, doi:10.1016/j.scitotenv.2009.09.015, 2009.

718 Keyte, I. J., Harrison, R. M., and Lammel, G.: Chemical reactivity and long-range transport
719 potential of polycyclic aromatic hydrocarbons - a review, *Chemical Society Reviews*, 42,
720 9333-9391, doi:10.1039/c3cs60147a, 2013.

721 Khairy, M., Muir, D., Teixeira, C., and Lohmann, R.: Spatial Trends, Sources, and Air-Water
722 Exchange of Organochlorine Pesticides in the Great Lakes Basin Using Low Density
723 Polyethylene Passive Samplers, *Environ. Sci. Technol.*, 48, 9315-9324,
724 doi:10.1021/es501686a, 2014.

725 Komprda, J., Komprdova, K., Sanka, M., Mozny, M., and Nizzetto, L.: Influence of Climate and
726 Land Use Change on Spatially Resolved Volatilization of Persistent Organic Pollutants (POPs)
727 from Background Soils, *Environ. Sci. Technol.*, 47, 7052-7059, doi:10.1021/es30437134,
728 2013.

729 Kurt-Karakus, P. B., Bidleman, T. F., Staebler, R. M., and Jones, K. C.: Measurement of DDT
730 fluxes from a historically treated agricultural soil in Canada, *Environ. Sci. Technol.*, 40,
731 4578-4585, doi: 10.1021/Es060216m, 2006.

732 Law, S. A., Diamond, M. L., Helm, P. A., Jantunen, L. M., and Alaei, M.: Factors affecting the
733 occurrence and enantiomeric degradation of hexachlorocyclohexane isomers in northern and
734 temperate aquatic systems, *Environ. Toxicol. Chem.*, 20, 2690-2698, 2001.

735 Leys, N. M., Ryngaert, A., Bastiaens, L., Top, E. M., Verstraete, W., and Springael, D.: Culture
736 Independent Detection of *Sphingomonas* sp. EPA 505 Related Strains in Soils Contaminated
737 with Polycyclic Aromatic Hydrocarbons (PAHs), *Microb. Ecol.*, 49, 443-450, 2005.

738 Li, C. L., Kang, S. C., Chen, P. F., Zhang, Q. G., and Fang, G. C.: Characterizations of
739 particle-bound trace metals and polycyclic aromatic hydrocarbons (PAHs) within Tibetan
740 tents of south Tibetan Plateau, China, *Environ Sci Pollut Res*, 19, 1620-1628,
741 doi:10.1007/s11356-011-0678-y, 2012.

742 Li, C. L., Bosch, C., Kang, S. C., Andersson, A., Chen, P. F., Zhang, Q. G., Cong, Z. Y., Chen, B.,
743 Qin, D. H., and Gustafsson, O.: Sources of black carbon to the Himalayan-Tibetan Plateau
744 glaciers, *Nature Communications*, 7, doi: 10.1038/Ncomms12574, 2016.

745 Li, J., Zhu, T., Wang, F., Qiu, X. H., and Lin, W. L.: Observation of organochlorine pesticides in
746 the air of the Mt. Everest region, *Ecotoxicol. Environ. Saf.*, 63, 33-41, doi:
747 10.1016/j.ecoenv.2005.04.001, 2006.

748 Liu, X., and Chen, B.: Climatic warming in the Tibetan Plateau during recent decades,
749 *International Journal of Climatology*, 20, 1729-1742, 2000.

750 Liu, X. B., Yao, T. D., Kang, S. C., Jiao, N. A. Z., Zeng, Y. H., and Liu, Y. Q.: Bacterial
751 Community of the Largest Oligosaline Lake, Namco on the Tibetan Plateau, *Geomicrobiol. J.*,
752 27, 669-682, doi: 10.1080/01490450903528000, 2010.

753 Liu, Y. Q., Yao, T. D., Jiao, N. Z., Kang, S. C., Xu, B. Q., Zeng, Y. H., Huang, S. J., and Liu, X. B.:
754 Bacterial diversity in the snow over Tibetan Plateau Glaciers, *Extremophiles*, 13, 411-423,
755 doi:10.1007/s00792-009-0227-5, 2009.

756 Liu, Y. Q., Yao, T. D., Jiao, N. Z., Liu, X. B., Kang, S. C., and Luo, T. W.: Seasonal Dynamics of
757 the Bacterial Community in Lake Namco, the Largest Tibetan Lake, *Geomicrobiol. J.*, 30,
758 17-28, doi:10.1080/01490451.2011.638700, 2013.

759 Lohmann, R., Gioia, R., Jones, K. C., Nizzetto, L., Temme, C., Xie, Z., Schulz-Bull, D., Hand, I.,
760 Morgan, E., and Jantunen, L.: Organochlorine Pesticides and PAHs in the Surface Water and
761 Atmosphere of the North Atlantic and Arctic Ocean, *Environ. Sci. Technol.*, 43, 5633-5639,
762 doi: 10.1021/Es901229k, 2009.

763 Ma, J. M., Hung, H. L., Tian, C., and Kallenborn, R.: Revolatilization of persistent organic
764 pollutants in the Arctic induced by climate change, *Nature Climate Change*, 1, 255-260, doi:
765 10.1038/Nclimate1167, 2011.

766 Ma, Y. G., Lei, Y. D., Xiao, H., Wania, F., and Wang, W. H.: Critical Review and Recommended
767 Values for the Physical-Chemical Property Data of 15 Polycyclic Aromatic Hydrocarbons at
768 25 degrees C, *J. Chem. Eng. Data.*, 55, 819-825, doi: 10.1021/Je900477x, 2010.

769 Ma, Y. X., Xie, Z. Y., Yang, H. Z., Moller, A., Halsall, C., Cai, M. H., Sturm, R., and Ebinghaus,
770 R.: Deposition of polycyclic aromatic hydrocarbons in the North Pacific and the Arctic, *J.*
771 *Geophys. Res.*, 118, 5822-5829, doi:10.1002/jgrd.50473, 2013.

772 Mulder, M. D., Heil, A., Kukucka, P., Klanova, J., Kuta, J., Prokes, R., Sprovieri, F., and Lammel,
773 G.: Air-sea exchange and gas-particle partitioning of polycyclic aromatic hydrocarbons in the
774 Mediterranean, *Atmospheric Chemistry and Physics*, 14, 8905-8915,
775 doi:10.5194/acp-14-8905-2014, 2014.

776 Nizzetto, L., Lohmann, R., Gioia, R., Jahnke, A., Temme, C., Dachs, J., Herckes, P., Di, G. A., and
777 Jones, K. C.: PAHs in air and seawater along a North-South Atlantic transect: trends,
778 processes and possible sources, *Environ. Sci. Technol.*, 42, 1580-1585, 2008.

779 Noyes, P. D., McElwee, M. K., Miller, H. D., Clark, B. W., Van Tiem, L. A., Walcott, K. C., Erwin,
780 K. N., and Levin, E. D.: The toxicology of climate change: Environmental contaminants in a
781 warming world, *Environ. Int.*, 35, 971-986, doi:10.1016/j.envint.2009.02.006, 2009.

782 Ridal, J. J., Bidleman, T. F., Kerman, B. R., Fox, M. E., and Strachan, W. M. J.: Enantiomers of
783 alpha-hexachlorocyclohexane as tracers of air-water gas exchange in Lake Ontario, *Environ.*
784 *Sci. Technol.*, 31, 1940-1945, doi: 10.1021/Es9607244, 1997.

785 Ruzickova, P., Klanova, J., Cupr, P., Lammel, G., and Holoubek, I.: An assessment of air-soil
786 exchange of polychlorinated biphenyls and organochlorine pesticides across Central and
787 Southern Europe, *Environ. Sci. Technol.*, 42, 179-185, doi: 10.1021/Es071406f, 2008.

788 Sheng, J. J., Wang, X. P., Gong, P., Joswiak, D. R., Tian, L. D., Yao, T. D., and Jones, K. C.:
789 Monsoon-driven transport of organochlorine pesticides and polychlorinated biphenyls to the
790 tibetan plateau: three year atmospheric monitoring study, *Environ. Sci. Technol.*, 47,
791 3199-3208, doi:10.1021/es305201s, 2013.

792 Spivakovsky, C. M., Logan, J. A., Montzka, S. A., Balkanski, Y. J., Foreman-Fowler, M., Jones, D.
793 B. A., Horowitz, L. W., Fusco, A. C., Brenninkmeijer, C. A. M., and Prather, M. J.:

794 Three-dimensional climatological distribution of tropospheric OH: Update and evaluation,
795 *Journal of Geophysical Research Atmospheres*, 105, 8931–8980, 2000.

796 Stemmler, I., and Lammel, G.: Cycling of DDT in the global environment 1950-2002: World
797 ocean returns the pollutant, *Geophys. Res. Lett.*, 36, doi:10.1029/2009GL041340, 2009.

798 Su, Y. S., Hung, H., Blanchard, P., Patton, G. W., Kallenborn, R., Konoplev, A., Fellin, P., Li, H.,
799 Geen, C., Stern, G., Rosenberg, B., and Barrie, L. A.: A circumpolar perspective of
800 atmospheric organochlorine pesticides (OCPs): Results from six Arctic monitoring stations in
801 2000-2003, *Atmos. Environ.*, 42, 4682-4698, doi:10.1016/j.atmosenv.2008.01.054, 2008.

802 Su, Y. S., Hung, H., Blanchard, P., Patton, G. W., Kallenborn, R., Konoplev, A., Fellin, P., Li, H.,
803 Geen, C., Stern, G., Rosenberg, B., and Barrie, L. A.: Spatial and seasonal variations of
804 hexachlorocyclohexanes (HCHs) and hexachlorobenzene (HCB) in the Arctic atmosphere,
805 *Environ. Sci. Technol.*, 40, 6601-6607, doi: 10.1021/Es061065q, 2006.

806 Tranvik, L. J., Downing, J. A., Cotner, J. B., Loiselle, S. A., Striegl, R. G., Ballatore, T. J., Dillon,
807 P., Finlay, K., Fortino, K., Knoll, L. B., Kortelainen, P. L., Kutser, T., Larsen, S., Laurion, I.,
808 Leech, D. M., McCallister, S. L., McKnight, D. M., Melack, J. M., Overholt, E., Porter, J. A.,
809 Prairie, Y., Renwick, W. H., Roland, F., Sherman, B. S., Schindler, D. W., Sobek, S.,
810 Tremblay, A., Vanni, M. J., Verschoor, A. M., von Wachenfeldt, E., and Weyhenmeyer, G. A.:
811 Lakes and reservoirs as regulators of carbon cycling and climate, *Limnol. Oceanogr.*, 54,
812 2298-2314, doi: 10.4319/lo.2009.54.6_part_2.2298, 2009.

813 Tremolada, P., Villa, S., Bazzarin, P., Bizzotto, E., Comolli, R., and Vighi, M.: POPs in Mountain
814 Soils from the Alps and Andes: Suggestions for a ‘Precipitation Effect’ on Altitudinal
815 Gradients, *Water Air & Soil Pollution*, 188, 93-109, 2008.

816 Venier, M., Dove, A., Romanak, K., Backus, S., and Hites, R.: Flame Retardants and Legacy
817 Chemicals in Great Lakes’ Water, *Environ. Sci. Technol.*, 48, 9563-9572,
818 doi:10.1021/es501509r, 2014.

819 Vilanova, R. M., Fernandez, P., Martinez, C., and Grimalt, J. O.: Polycyclic aromatic
820 hydrocarbons in remote mountain lake waters, *Water Res.*, 35, 3916-3926, doi:
821 10.1016/S0043-1354(01)00113-0, 2001.

822 Wang, C. F., Wang, X. P., Gong, P., and Yao, T. D.: Polycyclic aromatic hydrocarbons in surface
823 soil across the Tibetan Plateau: Spatial distribution, source and air-soil exchange, *Environ.*
824 *Pollut.*, 184, 138-144, doi:10.1016/j.envpol.2013.08.029, 2014.

825 Wang, J. B., Zhu, L. P., Daut, G., Ju, J. T., Lin, X., Wang, Y., and Zhen, X. L.: Investigation of
826 bathymetry and water quality of Lake Nam Co, the largest lake on the central Tibetan Plateau,
827 China, *Limnology*, 10, 149-158, doi:10.1007/s10201-009-0266-8, 2009.

828 Wang, X. P., Gong, P., Wang, C. F., Ren, J., and Yao, T. D.: A review of current knowledge and
829 future prospects regarding persistent organic pollutants over the Tibetan Plateau, *Sci. Total*
830 *Environ.*, 573, 139-154, doi: org/10.1016/j.scitotenv.2016.08.107, 2016.

831 Wang, X. P., Sheng, J. J., Gong, P., Xue, Y. G., Yao, T. D., and Jones, K. C.: Persistent organic
832 pollutants in the Tibetan surface soil: Spatial distribution, air-soil exchange and implications
833 for global cycling, *Environ. Pollut.*, 170, 145-151, doi: 10.1016/j.envpol.2012.06.012, 2012.

834 Wang, X. P., Gong, P., Sheng, J. J., Joswiak, D. R., and Yao, T. D.: Long-range atmospheric
835 transport of particulate Polycyclic Aromatic Hydrocarbons and the incursion of aerosols to
836 the southeast Tibetan Plateau, *Atmos. Environ.*, 115, 124-131,
837 doi:10.1016/j.atmosenv.2015.04.050, 2015.

838 Wania, F., Axelman, J., and Broman, D.: A review of processes involved in the exchange of
839 persistent organic pollutants across the air-sea interface, *Environ. Pollut.*, 102, 3-23, doi:
840 10.1016/S0269-7491(98)00072-4, 1998a.

841 Wania, F., Haugen, J. E., Lei, Y. D., and Mackay, D.: Temperature dependence of atmospheric
842 concentrations of semivolatile organic compounds, *Environ. Sci. Technol.*, 32, 1013-1021,
843 doi: 10.1021/Es970856c, 1998b.

844 Wania, F., Hoff, J. T., Jia, C. Q., and Mackay, D.: The effects of snow and ice on the
845 environmental behaviour of hydrophobic organic chemicals, *Environ. Pollut.*, 102, 25-41, doi:
846 10.1016/S0269-7491(98)00073-6, 1998c.

847 Wilkinson, A. C., Kimpe, L. E., and Blais, J. M.: Air-water gas exchange of chlorinated pesticides
848 in four lakes spanning a 1,205 meter elevation range in the Canadian Rocky Mountains,
849 *Environ. Toxicol. Chem.*, 24, 61-69, doi: 10.1897/04-071r.1, 2005.

850 Wong, F., Jantunen, L. M., Pucko, M., Papakyriakou, T., Staebler, R. M., Stern, G. A., and
851 Bidleman, T. F.: Air-Water Exchange of Anthropogenic and Natural Organohalogenes on
852 International Polar Year (IPY) Expeditions in the Canadian Arctic, *Environ. Sci. Technol.*, 45,
853 876-881, doi: 10.1021/Es1018509, 2011.

854 Wu, Y. H., Zheng, H. X., Zhang, B., Chen, D. M., and Lei, L. P.: Long-Term Changes of Lake
855 Level and Water Budget in the Nam Co Lake Basin, Central Tibetan Plateau, *Journal of*
856 *Hydrometeorology*, 15, 1312-1322, doi:10.1175/Jhm-D-13-093.1, 2014.

857 Xiao, H., Kang, S. C., Zhang, Q. G., Han, W. W., Loewen, M., Wong, F., Hung, H., Lei, Y. D., and
858 Wania, F.: Transport of semivolatile organic compounds to the Tibetan Plateau: Monthly
859 resolved air concentrations at Nam Co, *J. Geophys. Res.*, 115, doi: 10.1029/2010jd013972,
860 2010.

861 Xiao, Q. Y., Saikawa, E., Yokelson, R. J., Chen, P. F., Li, C. L., and Kang, S. C.: Indoor air
862 pollution from burning yak dung as a household fuel in Tibet, *Atmos. Environ.*, 102, 406-412,
863 doi:10.1016/j.atmosenv.2014.11.060, 2015.

864 Yang, R. Q., Xie, T., An, L., Yang, H., Turner, S., Wu, G., and Jing, C.: Sedimentary records of
865 polycyclic aromatic hydrocarbons (PAHs) in remote lakes across the Tibetan Plateau,
866 *Environ. Pollut.*, 214, 1-7, 2016.

867 Yao, T. D., Thompson, L. G., Mosbrugger, V., Zhang, F., Ma, Y., Luo, T., Xu, B. Q., Yang, X.,
868 Joswiak, D. R., Wang, W., Joswiak, M. E., Devkota, L. P., Tayal, S., Jilani, R., and Fayziev,
869 R.: Third Pole Environment (TPE), *Environmental Development*, 3, 52-64,
870 doi:10.1016/j.envdev.2012.04.002, 2012.

871 Zhang, G., Chakraborty, P., Li, J., Sampathkumar, P., Balasubramanian, T., Kathiresan, K.,
872 Takahashi, S., Subramanian, A., Tanabe, S., and Jones, K. C.: Passive Atmospheric Sampling
873 of Organochlorine Pesticides, Polychlorinated Biphenyls, and Polybrominated Diphenyl
874 Ethers in Urban, Rural, and Wetland Sites along the Coastal Length of India, *Environ. Sci.*
875 *Technol.*, 42, 8218-8223, doi: 10.1021/Es8016667, 2008.

876 Zhang, G. Q., Yao, T. D., Xie, H. J., Zhang, K. X., and Zhu, F. J.: Lakes' state and abundance
877 across the Tibetan Plateau, *Chin. Sci. Bull.*, 59, 3010-3021, doi:10.1007/s11434-014-0258-x,
878 2014.

879 Zhang, W. L., Zhang, G., Qi, S. H. and Peng, P. A.: A preliminary study of
880 organochlorinepesticides in water and sediments from two Tibetan Lakes. *Geochimica*. 32 (4),
881 363-367 (in Chinese with English abstract), 2003.

882

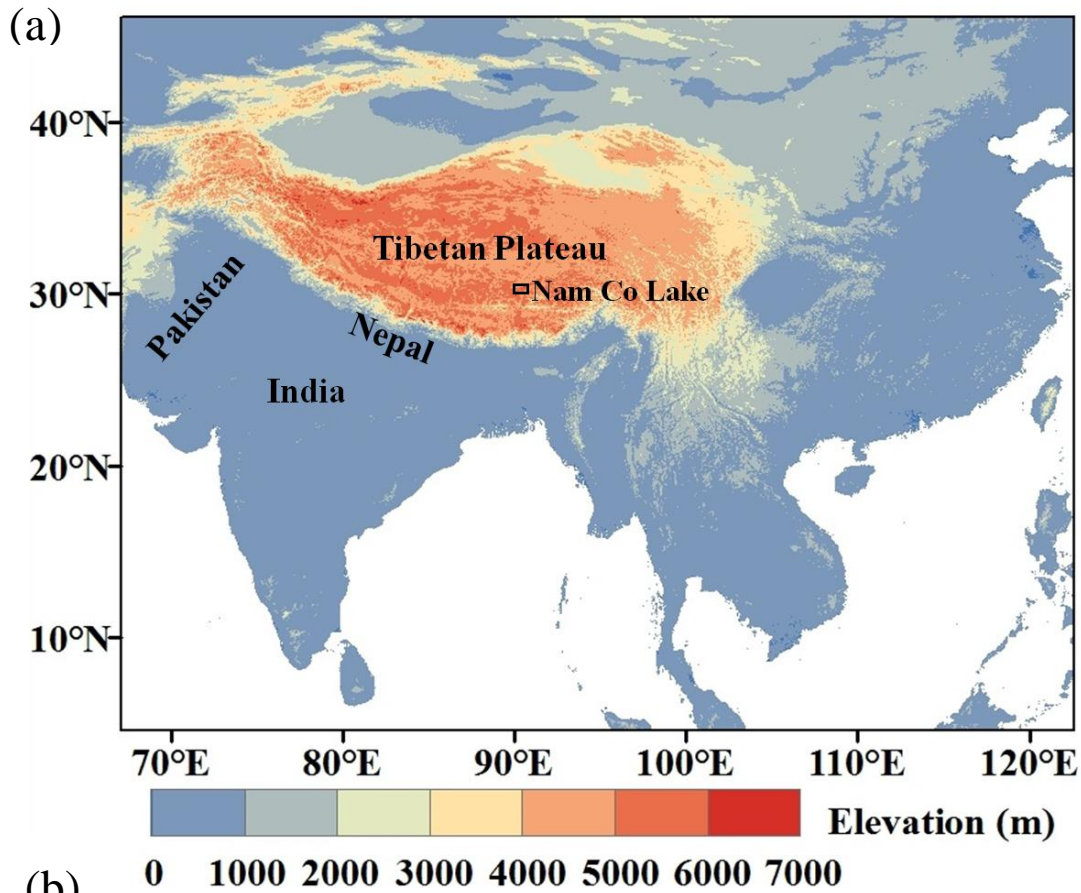
Table 1. Estimated fluxes ($\text{ng m}^{-2} \text{ day}^{-1}$) of air-water gas exchange (F_{AW}), atmospheric degradation (F_{deg}), dry deposition (F_{DD}), and wet deposition (F_{WD}) for individual PAHs during the ablation period and frozen periods, respectively.

883

| PAH | ablation period | | | | PAH | frozen period | | |
|---------------------------------|-----------------|------------------|-----------------|-----------------|-------------------|------------------|-----------------|-----------------|
| | F_{AW} | F_{deg} | F_{DD} | F_{WD} | | F_{deg} | F_{DD} | F_{WD} |
| Volatilization compounds | | | | | | | | |
| Acel | 80 ± 49 | 6 ± 5 | NA | -0.2 ± 0.1 | Acel | 1 ± 0.7 | -0.02 ± 0.001 | -0.03 ± 0.1 |
| Ace | 51 ± 19 | 4 ± 4 | -0.003 ± 0.002 | -0.4 ± 0.3 | Ace | 0.9 ± 0.5 | -0.01 ± 0.01 | -6 ± 5 |
| Flu | 203 ± 162 | 11 ± 8 | -0.1 ± 0.02 | -9 ± 7 | Flu | 1.8 ± 0.9 | -0.2 ± 0.2 | -43 ± 30 |
| sum | 335 | 21 | -0.1 | -9 | sum | 4 | -0.2 | -49 |
| Phe | -340 ± 604 | 82 ± 67 | -0.5 ± 0.1 | -42 ± 35 | Phe | 10 ± 4 | -2.2 ± 1.2 | -345 ± 237 |
| Ant | NA | 60 ± 63 | -0.04 ± 0.03 | -5 ± 5 | Ant | 4 ± 2 | -0.11 ± 0.05 | -16 ± 14 |
| Fla | NA | 5 ± 5 | -0.5 ± 0.1 | -20 ± 18 | Fla | 0.5 ± 0.3 | -4.6 ± 2.8 | -93 ± 64 |
| Deposition compounds | | | | | | | | |
| Pyr | -145 ± 154 | 20 ± 21 | -0.4 ± 0.1 | -18 ± 17 | Pyr | 2 ± 1 | -3 ± 1.5 | -128 ± 83 |
| BaA | -19 ± 23 | NA | -0.1 ± 0.1 | -3 ± 4 | BaA | NA | -1.1 ± 0.5 | -15 ± 10 |
| Chr | -54 ± 62 | 7 ± 8 | -0.5 ± 0.3 | -47 ± 56 | Chr | 0.2 ± 0.1 | -4.7 ± 2.3 | -19 ± 13 |
| Bbf | -5 ± 3 | 0.2 ± 0.1 | -0.6 ± 0.5 | -6 ± 5 | Bbf | 0.02 ± 0.01 | -2.2 ± 3.2 | -4 ± 8 |
| Bkf | -2 ± 1 | 0.2 ± 0.1 | -0.4 ± 0.4 | -2 ± 1 | Bkf | 0.1 ± 0.04 | -3.8 ± 1.9 | -8 ± 5 |
| Bap | -2 ± 1 | 0.2 ± 0.2 | -0.3 ± 0.5 | -3 ± 1 | Bap | 0.04 ± 0.03 | -4.7 ± 2.3 | -16 ± 10 |
| IcdP | -2 ± 1 | 0.7 ± 0.5 | NA | -2 ± 2 | IcdP | 0.1 ± 0.1 | NA | -3 ± 6 |
| DahA | -1 ± 0.7 | 0.1 ± 0.1 | NA | -0.1 ± 0.2 | DahA | 0.01 ± 0.01 | NA | -0.6 ± 1 |
| BghiP | -2 ± 0.4 | 0.02 ± 0.01 | -1 ± 1 | -3 ± 1 | BghiP | 0.01 ± 0.01 | -12 ± 6 | -6 ± 3 |
| sum | -231 | 28 | -3 | -85 | sum | 2 | -31 | -199 |
| Total PAHs | \ | 196 | -4.5 | -161 | Total PAHs | 20 | -38 | -702 |

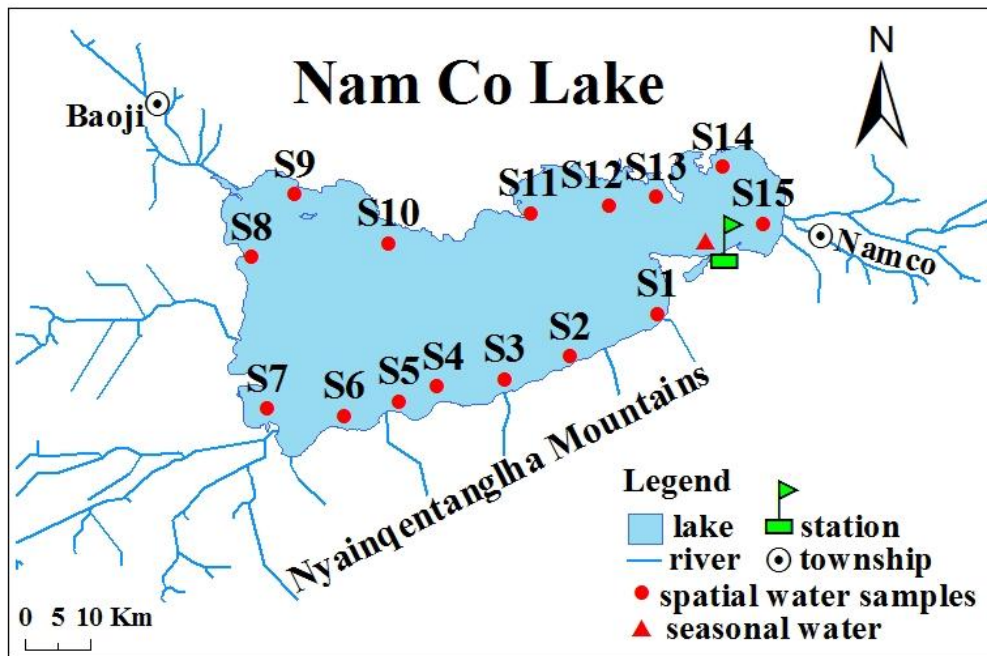
884

NA: not available; For F_{AW} , F_{DD} and F_{WD} , positive values indicate volatilization, and negative values indicate net deposition.



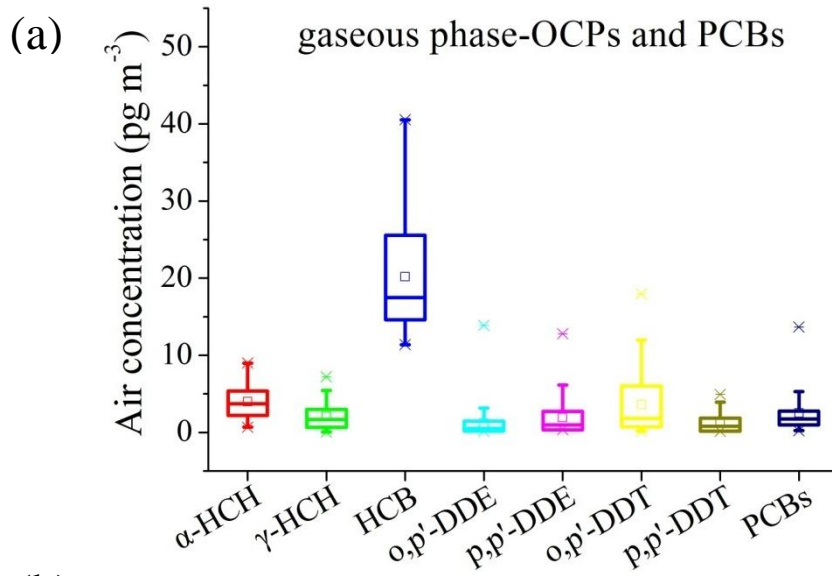
885

(b)

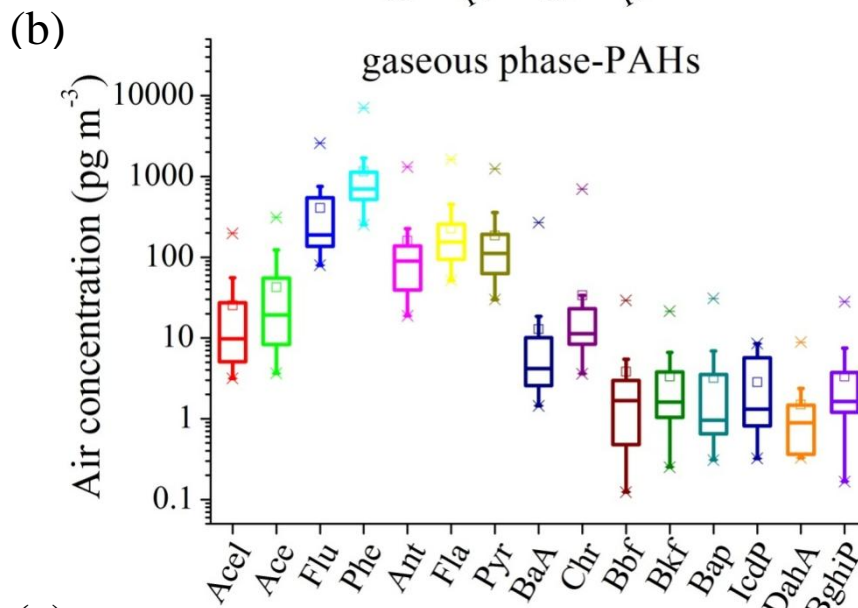


886

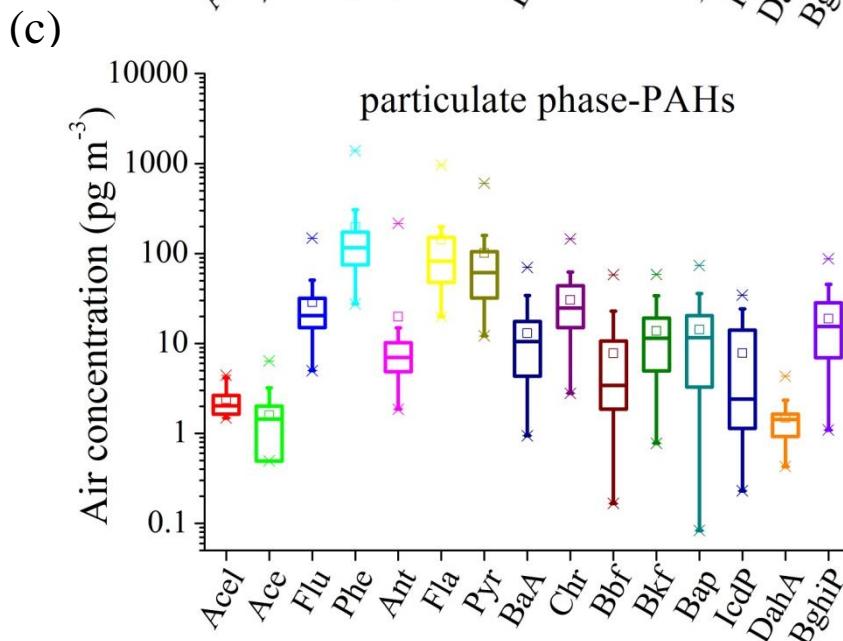
887 **Figure 1. Location of Nam Co Lake on the Tibetan Plateau (a) and the sampling**
 888 **sites for air and lake water (b). The station refers to the Nam Co Monitoring and**
 889 **Research Station, and it is also the air sampling site; S01 to S15 represent the 15**
 890 **sampling sites of surface water around the lake; the red triangle represents the**
 891 **sampling site of seasonal water from May to September.**



892



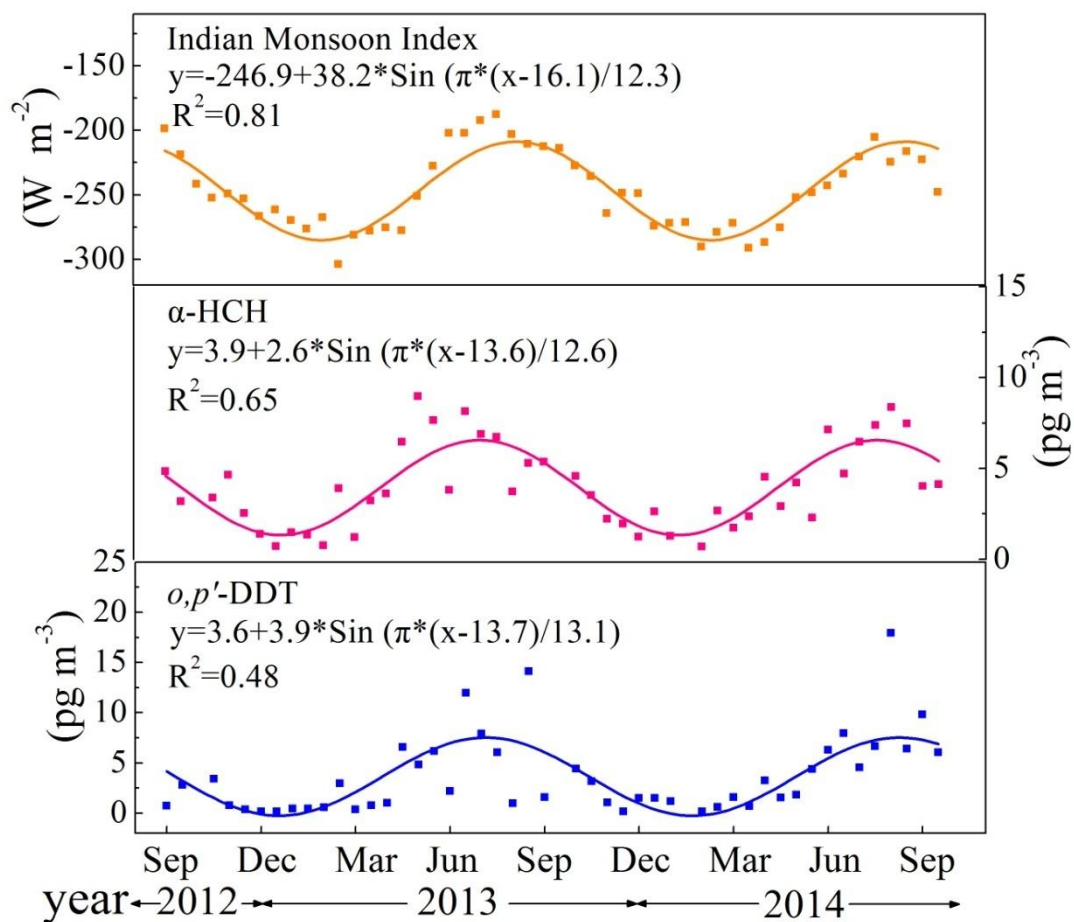
893



894

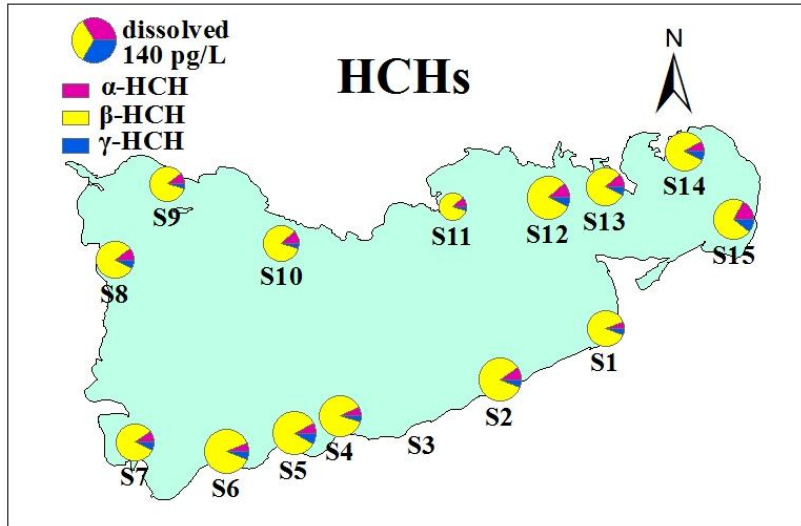
895 **Figure 2. Air concentrations of gaseous OCPs and PCBs (a), gaseous PAHs (b),**
 896 **and particulate phase PAHs (c) in Nam Co. The boxes are defined by the 25th**

897 **and 75th percentiles; whiskers mark the 10th and 90th percentiles; the median is**
898 **represented by a horizontal line; the mean by a square; and outliers with an**
899 **asterisk.**

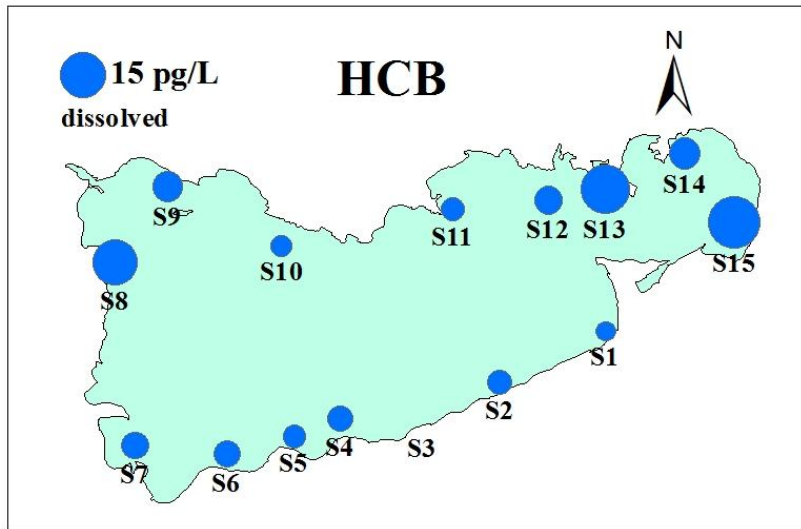


900

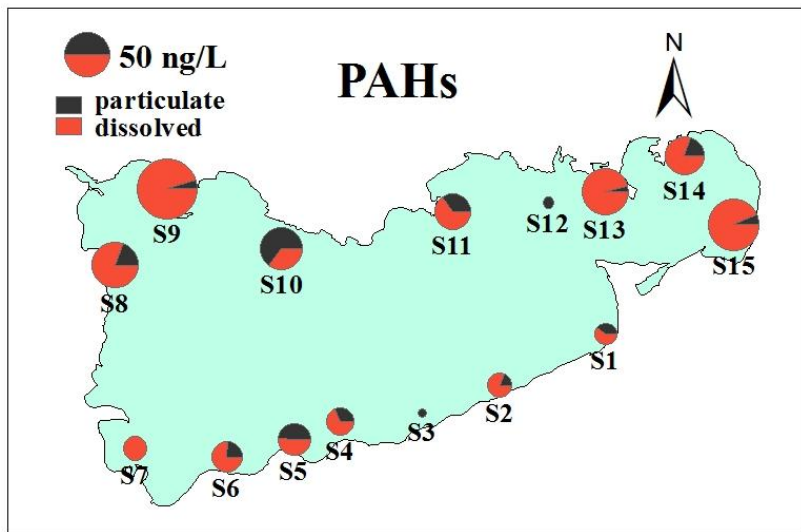
901 **Figure 3. Seasonal patterns of Indian Monsoon Index, the atmospheric**
 902 **concentrations of α -HCH and o,p' -DDT.**



903

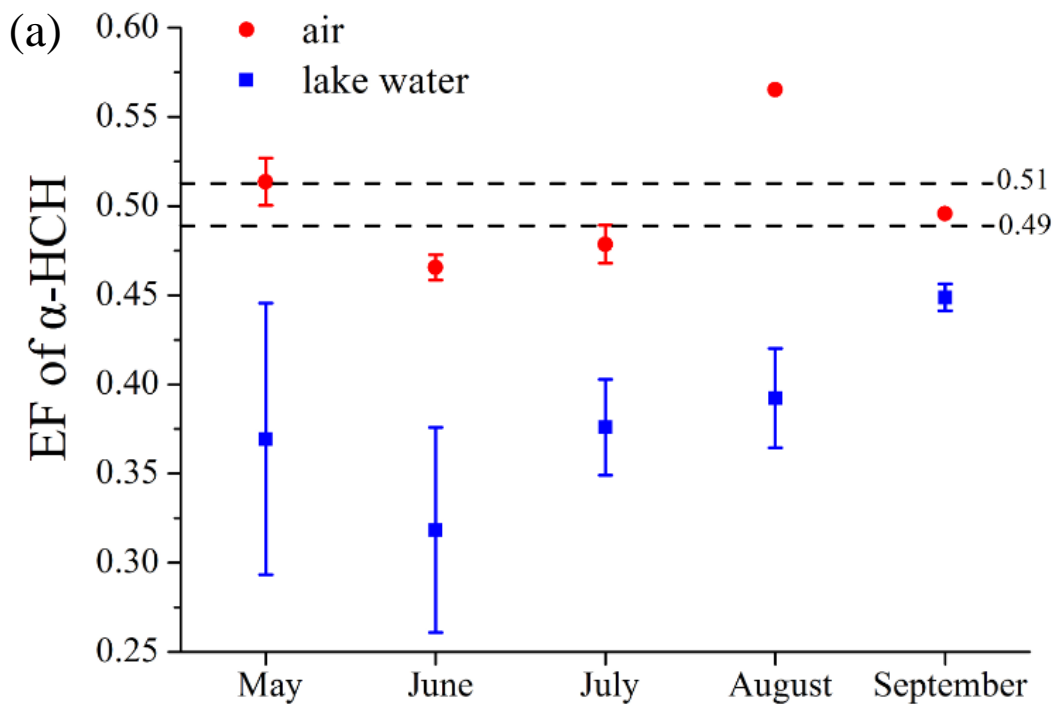


904

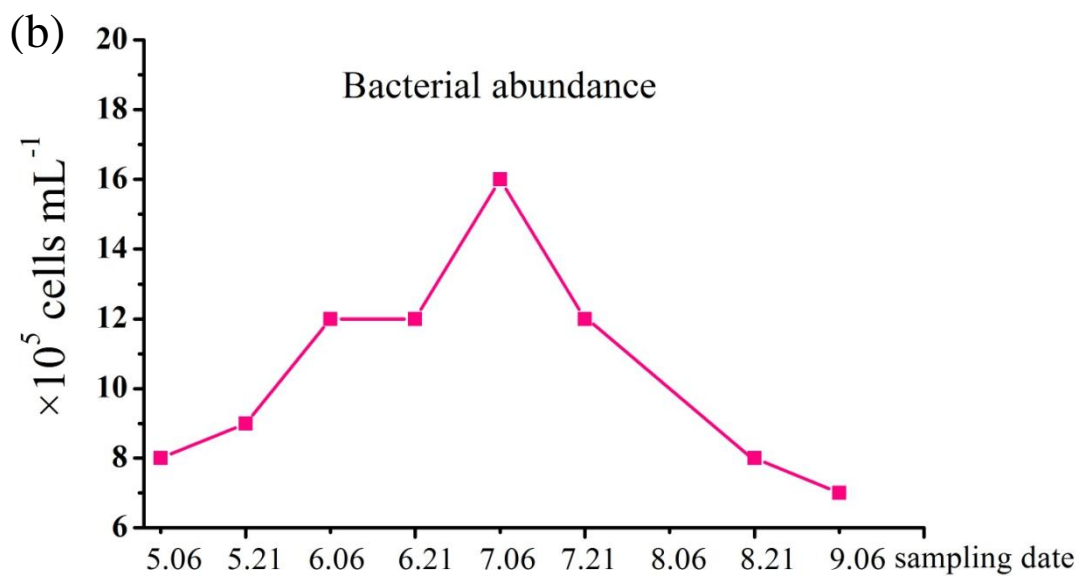


905

906 **Figure 4. Spatial distribution pattern of HCHs, HCB, and PAHs in the surface**
 907 **water of Nam Co Lake.**



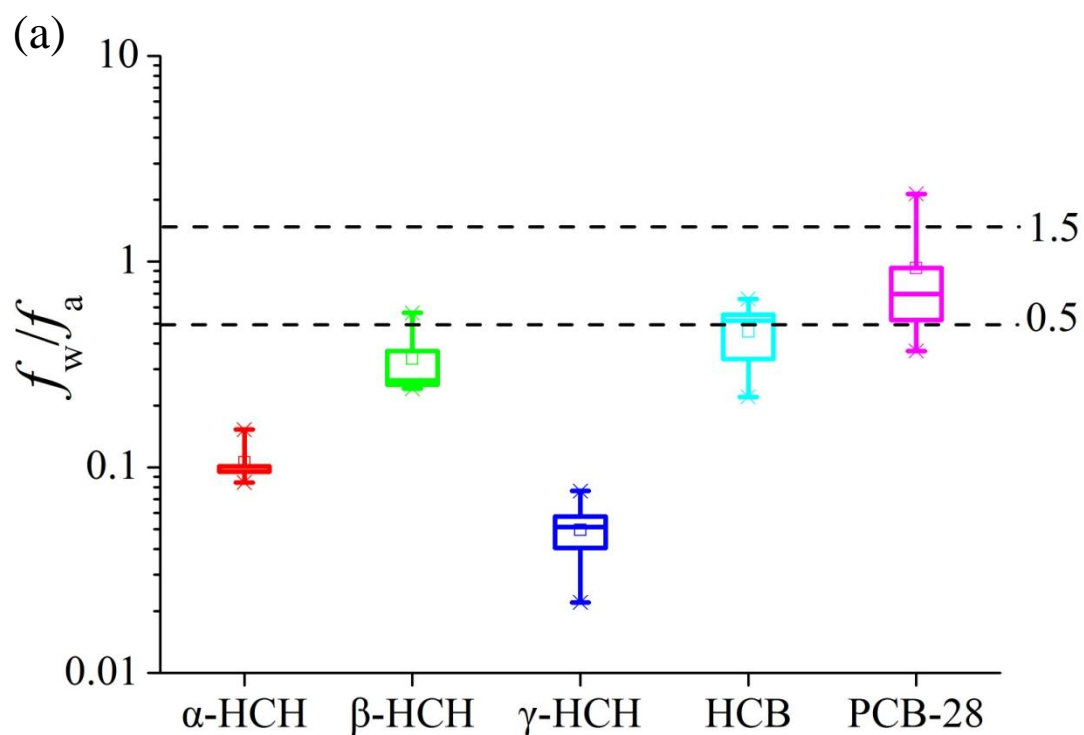
908



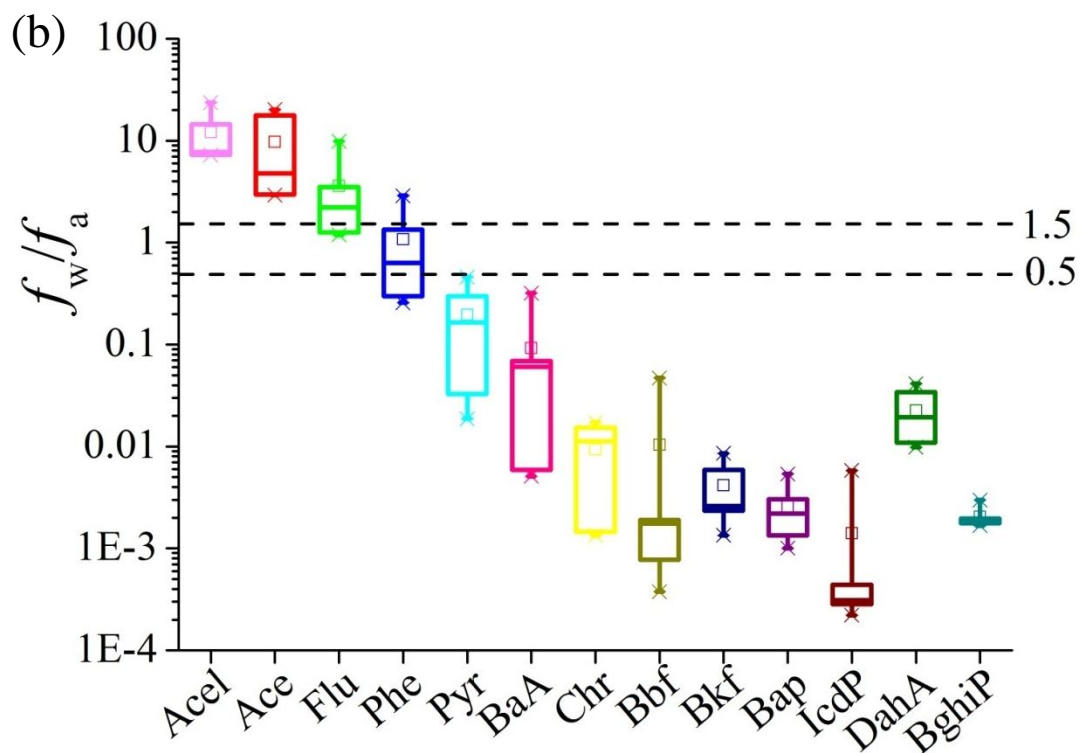
909

910 **Figure 5. Enantiomer fraction (EF) of α -HCH in the air and surface water from**
 911 **May to September (a), and the seasonal bacterial abundance in Nam Co Lake**
 912 **water (b). The data of bacterial abundance was derived from Liu et al. (2013),**
 913 **which represents the total bacteria in the lake surface water.**

914



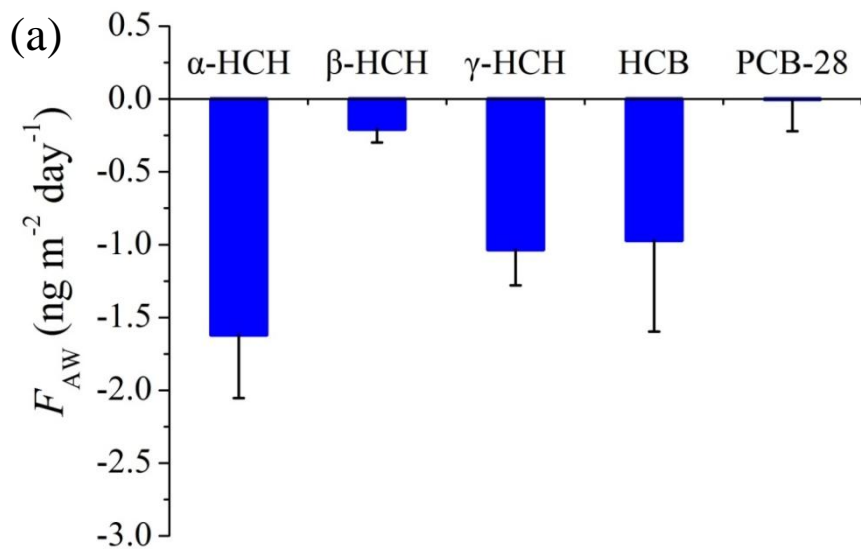
915



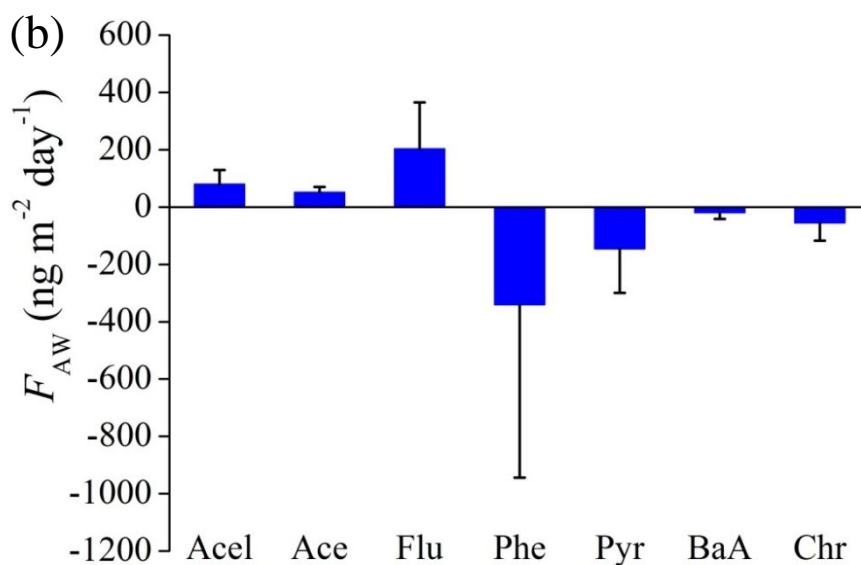
916

917 **Figure 6. Water/air fugacity ratios (f_w/f_a) for OCPs and PCB 28 (a), and**
918 **individual PAHs (b) in Nam Co Lake. The horizontal lines represent the**
919 **uncertainty range, 0.5-1.5 was considered as equilibrium.**

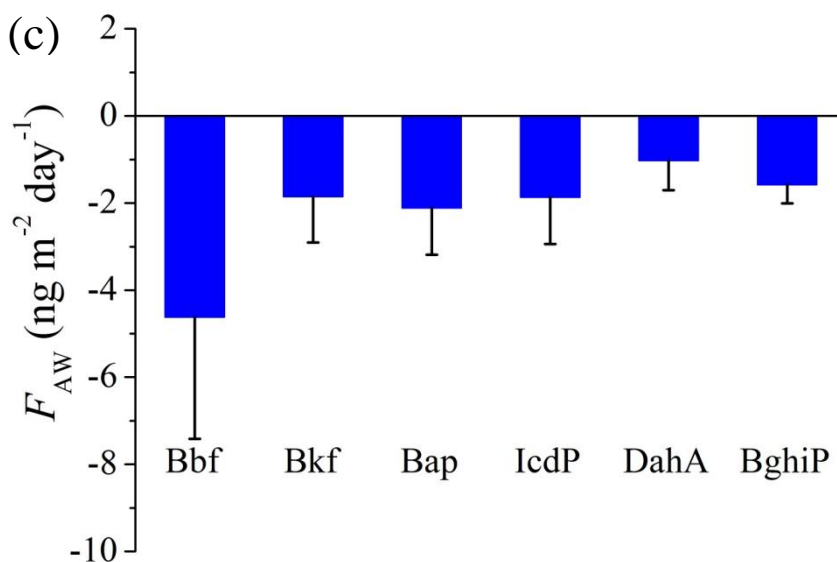
920



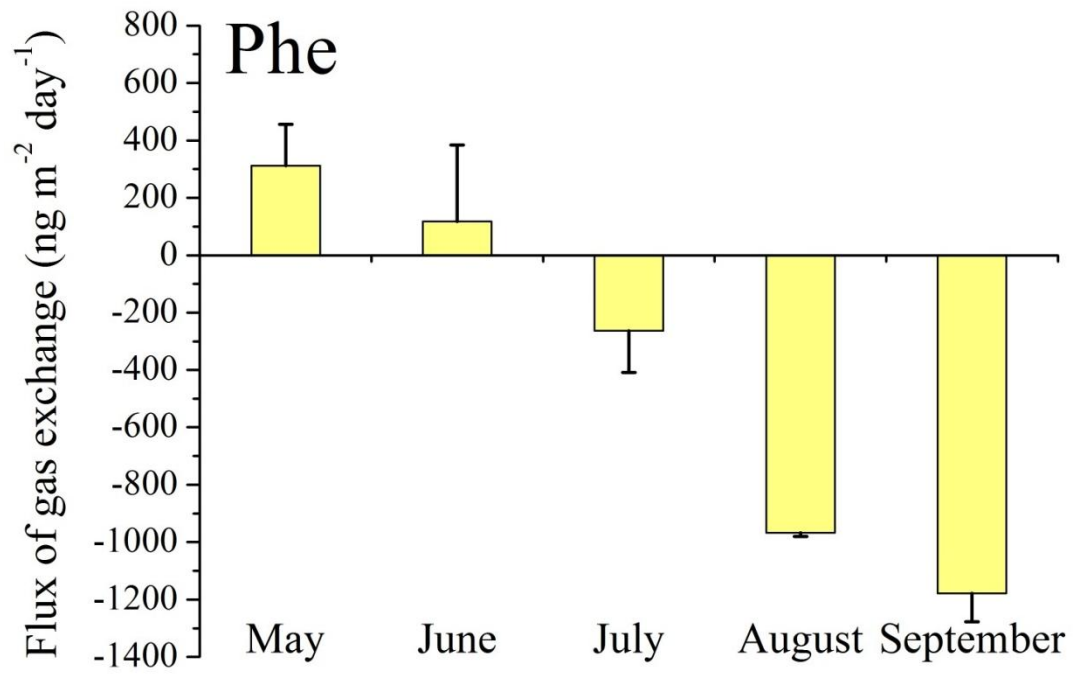
921



922



923 **Figure 7. Average air-water gas exchange fluxes (F_{AW}) for individual OCPs, PCB**
924 **28 (a), and PAHs (b, c) in Nam Co Lake. Positive values indicate net**
925 **volatilization, and negative values indicate net deposition.**



926

927

Figure 8. Reversal of the air-water gas exchange for Phe from May to September.